INTERNATIONAL GEOLOGY REVIEW, 2015
http://dx.doi.org/10.1080/00206814.2015.1114908

Taylor & Francis
Taylor & Francis Group

REVIEW

Outburst floods of the Maly Yenisei. Part I

Jigjidsurengiin Batbaatar and Alan R. Gillespie

Quaternary Research Center, University of Washington, Seattle, WA, USA

ABSTRACT

The Yenisei, the largest river flowing to the Arctic Ocean, repeatedly hosted cataclysmic floods during the Pleistocene. The largest of the known floods likely originated from palaeolakes in northern Mongolia, at the headwaters of the Little, or Maly, Yenisei. These ancient floods are among the greatest known globally. They left giant gravel dunes and wide abandoned channels in the Kyzyl basin, and high terraces in the gorges upstream. However, few detailed field studies of the flood deposits and no measurements of their ages have been made thus far. The largest palaeolakes were impounded during major glaciations by outlet glaciers from the East Sayan ice field in southern Siberia. The shorelines suggest four distinct palaeolake depths of 290, 175, 145, and 65 m. The timing and location of the glacier impounding the deepest lakes are uncertain but at its maximum, the Tengis outlet glacier was likely capable of impounding the 175 m lake. The dating of glacial deposits in and around the basin reveals that the maximum late Pleistocene glaciers were during Marine Oxygen Isotope Stage (MIS) 3. The ages for deep-lake sediments exposed in the basin behind the dam's location support this finding. During MIS 2 the Tengis glacier was large enough to impound at least the 145 m lake. However, the existence of a deep MIS 2 palaeolake in the basin has been challenged, because no evidence has been published of MIS 2 lake sediments from the cutbank outcrops and deep drilling cores. Additionally, the end moraines of the Tengis glacier, separated from the deeply eroded lateral moraines by the Maly Yenisei, remain undated; therefore it is uncertain exactly when this glacier crossed the river. This review is part I of a two-part article; Part II presents new age data to constrain the ages of the glacial dam.

ARTICLE HISTORY
Received 18 August 2015
Accepted 28 October 2015

KEYWORDS
Outburst floods; megafloods; cataclysmic floods; glacial dams; Maly Yenisei; Bolshoy Yenisei; palaeolake Darhad; Darhad basin; Sayan

1. Introduction

Modern geology originated more than two centuries ago, partly in response to the desire to find signs of the singular Biblical flood on the modern landscape (e.g. Montgomery 2013). The absence of widespread evidence for such a global flood and the principle of uniformitarianism expounded by Charles Lyell (Lyell 1830–3) put 'catastrophism' in disrepute, quelling the search for giant but infrequent floods for a century. This ended only with Bretz's (1923) recognition that huge, deep, and fast-moving floods reshaped the landscape in the Pacific Northwest (USA). These Missoula floods are now thought to have breached their ice-age glacial dams multiple times (Baker 1973; Waitt 1980), ending around 13.5 ka (e.g. Benito and O'Connor 2003). The geologic significance, wide geographic distribution, and number of large outburst floods modifying landscapes have become increasingly appreciated in recent decades (e.g. Malde 1968; Baker *et al*. 1993; Rudoy and Baker 1993; Komatsu *et al*. 1997; Grosswald 1999; Teller *et al*. 2002; Mangerud *et al*. 2004), and it is even suspected that they once coursed through Martian canyons (Baker and Milton 1974; Komatsu and Baker 2007).

Outburst floods originate in many ways (e.g. O'Connor *et al*. 2013), for example by the overtopping of sills impounding lakes or seas (e.g. Lake Bonneville, USA: Malde 1968; Bosporus, western Asia: Ryan *et al*. 1997), collapse of glacial or moraine dams (e.g. Palaeolake Missoula, USA: Pardee 1942; Yarlong Tsangpo, Tibet, Montgomery *et al*. 2004), or overtopping or erosion of landslide dams (e.g. Yigong Tsangpo, Tibet: Shang *et al*. 2003). Some, for example those from Lake Agassiz (Canada), arose multiple times from multiple causes over a period of a few thousand years during deglaciation of the Laurentide Ice Sheet (e.g. Fisher 2003 and references therein); others have occurred during modern times (e.g. Merzbacher Lake, Kyrgyz Tien Shan; Wortmann *et al*. 2014). Some of the greatest floods are summarized in Figure 1.

The impact of outburst floods on the landscape depends on the total discharge, the depth of the

CONTACT Jigjidsurengiin Batbaatar bataa@uw.edu

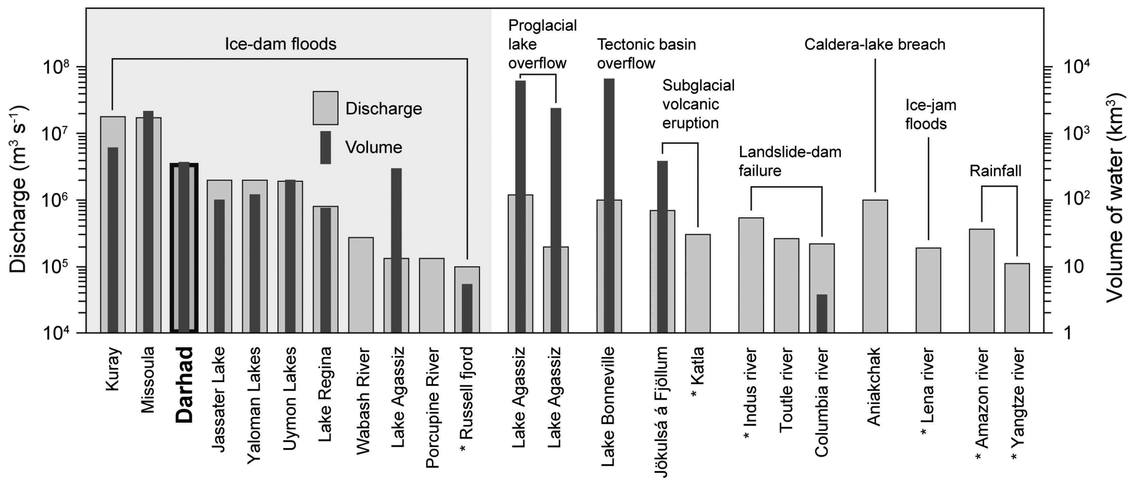

(* events in historic time)

Figure 1. Peak discharge and volume of released water from major Quaternary floods (modified after O'Connor and Costa 2004). The most energetic floods are outbursts from failed glacier dams. The values for the Darhad flood are from the 172 m-deep palaeolake impounded by the Tengis glacier. The outburst from the deepest palaeolake Darhad was more energetic (see text for details).

flood, the flow speed, and the sediment load entrained, as well as resistance of the landscape to erosion. The discharge rate depends on the speed with which the dam is breached, ice dams being eroded faster than bedrock sills. Floods with discharge rates exceeding 10^5 m^3 s^{-1} are termed 'catastrophic' (Komatsu *et al*. in this issue). The power of these floods are best demonstrated by the well-documented records of the floods from Palaeolake Missoula – the flood had a total volume of 2184 km^3 (Clarke *et al*. 1984), a depth of 550 m or more, and flow speeds as high as 36 m s^{-1}, with discharge rates of 17 × 10^6 m^3 s^{-1} (O'Connor and Baker 1992). The initial outburst of the Missoula floods at the end of the Last Glacial Maximum (LGM) is estimated to have transported at least 700 km^3 of eroded sediments to the ocean (Normark and Reid 2003). In their review of great floods and their mechanisms, O'Connor *et al*. (2013) concluded that the frequency of the floods was the major factor defining their ability to shape the landscape.

The major rivers of Siberia – among them the Ob, Yenisei, and Lena – all received outburst floods during the Pleistocene Epoch (Margold *et al*. 2011; Komatsu *et al*. in this issue). The Yenisei (Figure 2) is one of the largest rivers in the world (annual discharge: 573 km^3; length ~3500 km long; basin area: 2.6 × 10^6 km^2: Yang *et al*. 2004), yet its outburst floods have received less attention than floods with comparable significance elsewhere, such as the Missoula Floods and those from the Kuray, Chuya, and Katun basins of the upper Ob river (Table 1). In this article we consider some of the most catastrophic outburst floods yet studied, those of the upper reaches of the Yenisei river.

This article consists of two parts: (1) a review of relevant previous studies and (2) new data that resolve important questions posed by Krivonogov *et al*. (2012), who thoroughly summarized the literature on the history of a sequence of palaeolakes in Darhad basin. These palaeolakes were at the headwaters of the Maly Yenisei in northern Mongolia, one of the main tributaries of the Yenisei, and were the sources of the largest of the Yenisei floods (e.g. Komatsu *et al*. 2009). Here in part I we review the published evidence for the floods downstream of the palaeolakes and the glacial and sediment dams that impounded the Darhad palaeolakes, and the palaeolakes themselves. We have performed new photo interpretation of satellite images (Google Earth) of the Maly Yenisei between the Kyzyl and Darhad basins, and the results are intercalated into the review (Sections 2.2.2 and 2.2.3).

Age control for the palaeolakes has been provided by prior luminescence dating of lake sediments, ^{14}C dating of organic matter preserved in them, and ^{10}Be cosmic-ray exposure (CRE) dating of glacial deposits. The calibration curve for the ^{14}C dating has been revised recently with updated data sets. Therefore, we recalibrated the reported ^{14}C ages using the IntCal13 curve (Reimer *et al*. 2013) on the Calib 7.1 online calculator (Stuiver and Reimer 1993). Hereafter we refer only to these recalibrated ages (cal years BP). The ^{14}C dating studies are summarized in section 3.1.

Recent developments in CRE dating techniques have suggested that the spallation production rate of ^{10}Be was lower than of the early estimations (e.g. Balco *et al*. 2009; Putnam *et al*. 2010; Young *et al*. 2013). Accordingly, we recalculated all the literature ages

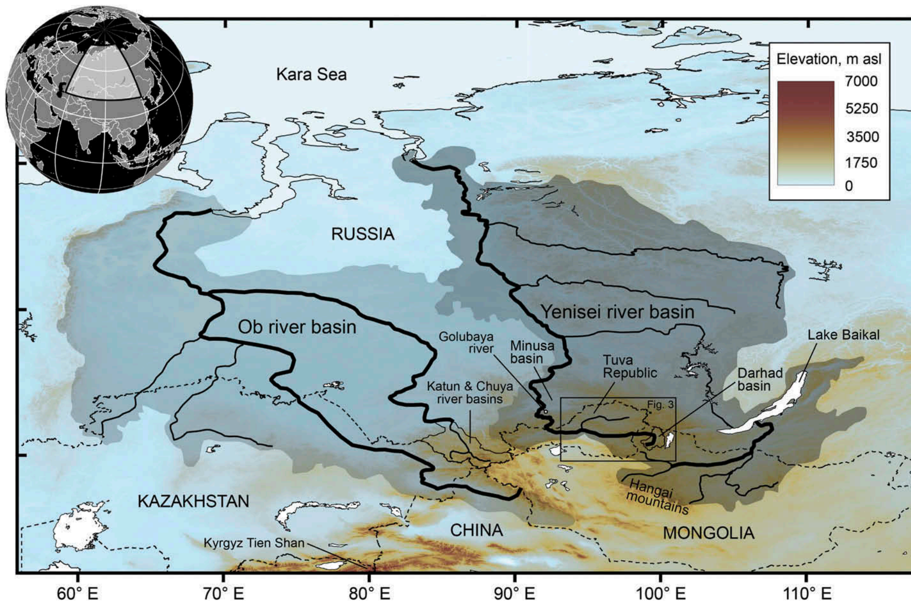

Figure 2. The largest Pleistocene floods in Siberia originated in the Kuray and Chuya basins and flowed into the Katun river (headwaters of the Ob river), and from Darhad basin (headwaters of the Yenisei river). In this figure the Kuray basin is included within the combined border for the Katun and Chuya river basins. Background: shaded-relief image produced from 90 m Shuttle Radar Topographic Mission (SRTM) elevation data (Farr *et al*. 2007).

Table 1. Selected large outburst floods from glacier-dammed lakes.

Name	Location	Peak discharge (10^6 m^3 s^{-1})	Lake depth (m)	Lake volume (km^3)	Reference
Kuray	Altai, Russia	18 10	–400	–607	Baker *et al*. (1993), Herget (2005)
Missoula	NW USA	17	375	2184	O'Connor and Baker (1992), Clarke *et al*. (1984), Craig (1987)
Darhad (1825 m asl[a])	Mongolia	>5.8[c]	287	809	Komatsu *et al*. (2009)
Darhad (1710 m asl[b])	Mongolia	3.5	172	373	Komatsu *et al*. (2009)
Yarlong Tsangpo	Tibet, China	1–5	680	832	Montgomery *et al*. (2004)
Matanuska River	Alaska, USA	2.0–3.3[d]	<110	500–1400	Wiedmer *et al*. (2010)

[a]Maximum highstand (Krivonogov *et al*. 2005; Gillespie *et al*. 2008), pre-LGM
[b]Local LGM maximum highstand (Gillespie *et al*. 2008; Komatsu *et al*. 2009)
[c]Estimate assuming velocity is no less than for the lower, modelled outburst (1710 m)
[d]Assuming dam-break origin; jökulhlaup origin would imply 0.15–0.27 × 10^6 m^3 s^{-1}

using globally calibrated ^{10}Be production rate of Heyman (2014). Hereafter we refer only to the recalculated ^{10}Be ages, and the summary of the CRE dating studies is provided in section 3.2.

1.1. Geographic names

Many of the pioneer studies in Siberia and northern Central Asia were reported in Russian. Local geographic names in the Evenki, Tuvan, and Mongolian languages were approximated by Russian pronunciation and recorded in Cyrillic script. Names cited in scientific literature are a mixture of the Russian and local names and they were transcribed from Cyrillic to Latin script. However, the Latin spellings of names and equivalents in the literature have been used inconsistently. In this article we have tried to use the most widely recognized, and we have summarized the local equivalents in Table 2a. We have translated generic geographic terms such as 'river' or 'lake' to English, and for clarity we added them in lower case where they are not part of the native name. Thus, the 'Yenisei' (a stand-alone name for the river) becomes the 'Yenisei river' if helpful, and the Sayan becomes the Sayan mountains. Common terms used in this article are listed along with the translations in Table 2b.

1.2. Geography of the Maly Yenisei river

Geographic features discussed in this paper are marked on a .kmz file (online supplementary material at http://dx.doi.org/10.1080/00206814.2015.1114908) that may be used with Google Earth. The Maly Yenisei (Figure 3) originates in the Ulaan Taiga mountains on the western

Table 2. Geographical names used in this article.

a. Spelling for common local names

This article	Alternative spelling(s)
Baikal	Baigal
Büsiin	Busein
Chuya	Chuja
Darhad	Darkhad, Darkhat, Darkhadyn
Högiin	Hogyin, Hogiin, Hugiin
Horidol	Khoridolyn
Hövsgöl	Kubsukul, Khovsgol
Kaa	Ka
Mönh Saridag	Monkh Saridag, Munku Saridag
Otgontenger	Otgon Tenger,
Shishhid	Shishged, Shishigt, Shishkit
Tengis	Tengissiin
Todzha	Todza
Tuva	Tyva
Yenisei	Yenesei, Yenisey

b. Generic terms and their transliterations

Geographical terms	Tuvan	Russian	Mongolian
river	khem	reka	gol
lake	khöl	ozero	nuur
depression, basin	-	kotlovina	hotgor
mountains	uula	khrebty	uul, nuruu

margin of Darhad basin in Mongolia, where the river is known as the Shishhid. The Maly Yenisei exits Darhad basin through a narrow gorge between the Ulaan Taiga and the East Sayan mountains, both of which supported ice caps during the Pleistocene glaciations (Figure 4), and flows west to the confluence with the north-flowing Büsiin and south-flowing Belin rivers, on the border between Mongolia and Tuva Republic of the Russian Federation. Downstream for ~80 km to a major confluence, the Maly Yenisei is known as the Kyzyl river (Figure 3). The north-flowing tributary is known as the Kaa river, and the combined flow retains this name downstream until the next major confluence, with the south-flowing Bolshoy Yenisei (or Bii river) at the city of Kyzyl, the Tuvan capital. The Bolshoy Yenisei drains the Todzha basin, itself the source of large outburst floods (Komatsu *et al*. 2009). Downstream from Kyzyl, the combined forks of the Yenisei are known as the Upper Yenisei, or Ulug river, until the river debouches from the West Sayan mountains into the Minusa basin (Figure 2), at elevation of 450 m above sea level (asl). Thereafter the Yenisei flows north ~2000 km to the Arctic Ocean. Local names for the tributaries of the Yenisei are summarized in Table 3 and shown in Figure 3.

2. Flood evidence on the Upper Yenisei

In this section we summarize the geomorphological and sedimentological features along the upper reaches of the Yenisei river that provide evidence for very large floods. Our review is primarily of the Maly Yenisei, but for context we also include the Ulug river and the Bolshoy Yenisei. The floods down the Bolshoy Yenisei arose from a number of sources (Komatsu *et al*. 2009); the floods along the Ulug and in the Minusa basin downstream arose from both the Bolshoy and Maly Yenisei, and records there should accordingly be more complex. In contrast, the floods on the Maly Yenisei upriver from the city of Kyzyl mainly originated at the river's headwaters in Darhad basin.

2.1. Palaeoflood and palaeolake evidence from adjacent basins

2.1.1. Evidence from the Minusa basin and Ulug river

After flowing through the narrow gorges of the West Sayan mountains, the Yenisei river debouches onto the broad flood plains in the Minusa basin. In the western and central part of the basin, at least two sets of braided

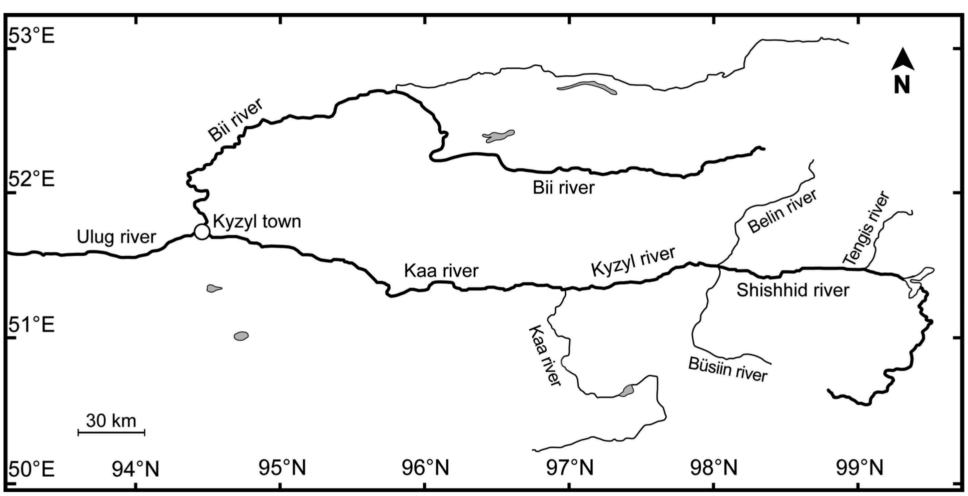

Figure 3. Major tributaries to the Yenisei river and their local names.

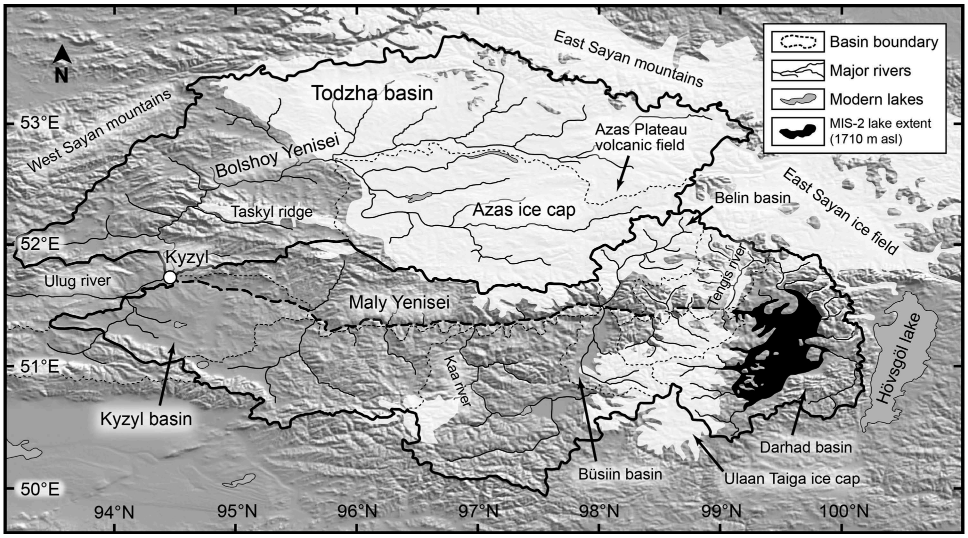

Figure 4. Basin and watershed map of the upper Yenisei river. Todzha basin collects water for the Bolshoy Yenisei river. The Maly Yenisei originates in Darhad basin and joins the Bolshoy Yenisei to form the Ulug river, the local name for the upper Yenisei. Outlet glaciers from the East Sayan ice field descended through the Tengis river valley and impounded large lakes in Darhad basin. The Pleistocene Azas ice cap occupied the Azas Plateau, which is also the location of the Azas Plateau volcanic field. Shaded-relief image produced from 90 m SRTM elevation data (Farr *et al.* 2007).

Table 3. Names of geographical features and their local variants.

Geographical name	Local name	Headwaters and basin
Yenisei	-	Lower and Upper Yenisei
Lower Yenisei	-	Nizhnaya and Podkamennaya Tunguska, Angara
Upper Yenisei	Ulug river	Bolshoy and Maly Yenisei
Bolshoy Yenisei	Bii river	Systyg river (Todzha basin)
Maly Yenisei	Kaa river, Kyzyl river, Shishhid river	Darhad basin

and/or anastomosing palaeochannels were identified from the satellite images by Komatsu *et al.* (2009). They proposed two alternatives for the origin of the palaeochannels: either by migration of streams or by high-energy floods. However, no chronology has been determined for these palaeochannels, they do not appear to have been studied in the field, and their origin could not be established decisively.

Komatsu *et al.* (2009) noted prominent high terraces in the mountains upstream from the Minusa basin. For example, there are ~10 m-high terraces of cross-bedded fluvial sediments along the Golubaya river (52.952583°N; 91.543167°E), near the city of Sayanogorsk, where sand beds alternate with layers of coarser sub-angular pebbles. Yamskikh *et al.* (2001) considered these sediments to be alluvial and lacustrine, deposited behind a temporary glacial dam, but Carling *et al.* (2002) and Rudoy (2002) likened the terraces to the giant bars in the Katun and Chuya river valleys at the headwaters of the Ob river. These were deposited during catastrophic outburst floods when there was an abrupt decrease in stream energy, for example on the lee sides of the bends of the main valleys. Komatsu *et al.* (2009) interpreted the sediments of these high terraces to have been formed from the suspended load of an energetic flood, accumulated when the floodwaters stagnated in tributary canyons.

Upstream of the Minusa basin and the West Sayan, the Upper Yenisei (Ulug river) flows through the Kyzyl basin, a broad plain that preserves evidences of giant flood events. Along the banks of the Ulug river in the Kyzyl basin are several hanging valleys ending in cliffs ~200 m high and flanking the main river. These indicate deep, erosive flow down the Ulug river that the smaller tributaries could not match. Rudoy (2002) and Komatsu *et al.* (2009) both attributed the hanging valleys to intense erosion during giant floods, observing that high-energy floods would have completely or largely eroded pre-existing fans at the mouths of these hanging valleys and prevented the tributaries from adjusting to the lowered base level.

Downstream from and near the confluence of the Bolshoy and Maly Yenisei, the unstudied chronology of flooding may be complex because the sources of the floodwaters may be from the different basins and timing of dam disruption may not have been synchronized. On the Maly Yenisei upstream of the confluence, Komatsu *et al*. (2009) suspected that the largest floods originated from Darhad basin, and the chronology of flood deposits and other features above the modern floodplain may be accordingly simpler. However, smaller floods from tributary streams (e.g. Komatsu *et al*. 2009) may complicate the detailed geologic record of the Maly Yenisei as well.

In the central part of the Kyzyl basin, south of the city of Kyzyl, two generations of northwest-trending linear features cover an area of ~1500 km^2, 45 km (NW–SE) × 33 km (NE–SW). Komatsu *et al*. (2009) suggested that these are aeolian dunes made of reworked flood sands from the Maly and Bolshoy Yenisei rivers.

2.1.2. Evidence from Bolshoy Yenisei

The Todzha basin in Tuva (Figure 4) is drained by the Bolshoy Yenisei. Although Komatsu *et al*. (2009) regarded the basin as a source of outburst floods, fieldwork there has not been completed and photo-reconnaissance has only been done at the resolution limits of available satellite remote-sensing data (75 m for Radarsat SCAN SAR: Raney *et al*. 1991; 30 m for Landsat TM: US Geological Survey 2012). Komatsu *et al*. (2009) admitted that as yet no clear cataclysmic flood indicators such as 'giant current ripples' (*sensu* Bretz 1969) or 'gravel dunes' (*sensu* Carling 1996) have been identified there, although there are some suggestive features near the Taskyl ridge. These include truncated tributary terraces, ~40 m above the Bolshoy Yenisei (51.949581°N; 94.407972°E), and a possible high terrace on an inside bend ~50 m above the river (52.321158°N; 94.584636°E). Another possible high terrace 5 km downstream from the others is likely the remnant of a landslide.

Although definitive outburst flood evidence has not been discovered, the Todzha basin hosted giant lakes at different times in the Quaternary. During Middle–Late Pleistocene time, lakes with depths of up to 250 m covered areas of ~2000 km^2 (volume: 310 km^3), and during the Late Pleistocene to Holocene there were smaller lakes with a maximum depth of 60 m (volume: 8 km^3) (Komatsu *et al*. 2009). Although these palaeolakes drained down the Bolshoy Yenisei, the rate is unknown and dependent on the dams that impounded them. Possible dams include glaciers, debris/landslides, ice jams in the river, and tectonic scarps (Yamskikh and Yamskikh 1999; Arzhannikov *et al*. 2000; Komatsu *et al*. 2009).

Dam failures are not the only possible mechanism for floods from the Todzha basin. The Todzha basin and the Azas Plateau hosted an ice cap (Figure 4) at times during the Pleistocene Epoch (Komatsu *et al*. 2007a), and Komatsu *et al*. (2007b) showed that subglacial volcanic eruptions occurred from several middle-late Pleistocene (Yarmolyuk *et al*. 2001) vents of the Azas Plateau volcanic field. These may have been capable of producing meltwater floods as occur today from the subglacial Grímsvötn volcano in Iceland (Jóhannesson 2002).

Some of the mechanisms suggested for impounding the Todzha palaeolakes appear to be improbable. For example, the continuous section of lacustrine sediments from the Middle–Late Pleistocene lake suggests continuous deposition over a long period of time (Komatsu *et al*. 2009), inconsistent with ice jams or glacier dams from the Taskyl ridge. In any case, the glaciers there appear to have terminated hundreds of metres above and at least 1 km from the river (Figure 4) and could not have impounded a 250 m-deep lake (Grosswald 1965). Komatsu *et al*. (2009) concluded that these lakes developed behind a 1100 m-high landslide block at the junction between the Bolshoy Yenisei and Krasnaya rivers (52.417683°N, 94.772517°E). If this is true, the release of water from the Todzha basin may not have been as sudden as for the floods down the Maly Yenisei, many of which were released from glacier dams. Therefore, the floodwater discharge rate along the Bolshoy Yenisei is likely to have been lower than for the Maly Yenisei floods, even if the released volumes (Table 1) were similar. Floodwaters in the Kyzyl basin and downstream could have originated from either the Todzha or Darhad basin, at the headwaters of the Maly Yenisei. Distinguishing flood sediments of Bolshoy and Maly Yenisei in the Kyzyl basin may require detailed study of the lithology and its chronology, and such studies have not yet been attempted.

2.2. Evidence from the Maly Yenisei

2.2.1. Large fluvial gravel dunes in the Kyzyl basin

In the Kyzyl basin upriver from the city of Kyzyl for ~100 km, inset terraces are locally preserved above the modern flood plain and incised by the Maly Yenisei. There are at least three levels: ~10, ~30–40, and ~40–50 m above the modern river (Figure 5). Tributary streams have cut through the higher terraces and grade to the lowest terrace, on which they have deposited small fans. At multiple locations (e.g. 51.683283°N, 94.684433°E, 670 m asl; 51.650583°N, 94.918383°E, 672 m asl), large gravel dunes are preserved on the second-lowest terrace (Figure 5). The highest benches, with smaller gravel dunes, are found at 690–700 m asl (e.g. 51.667817°N, 94.921817°E).

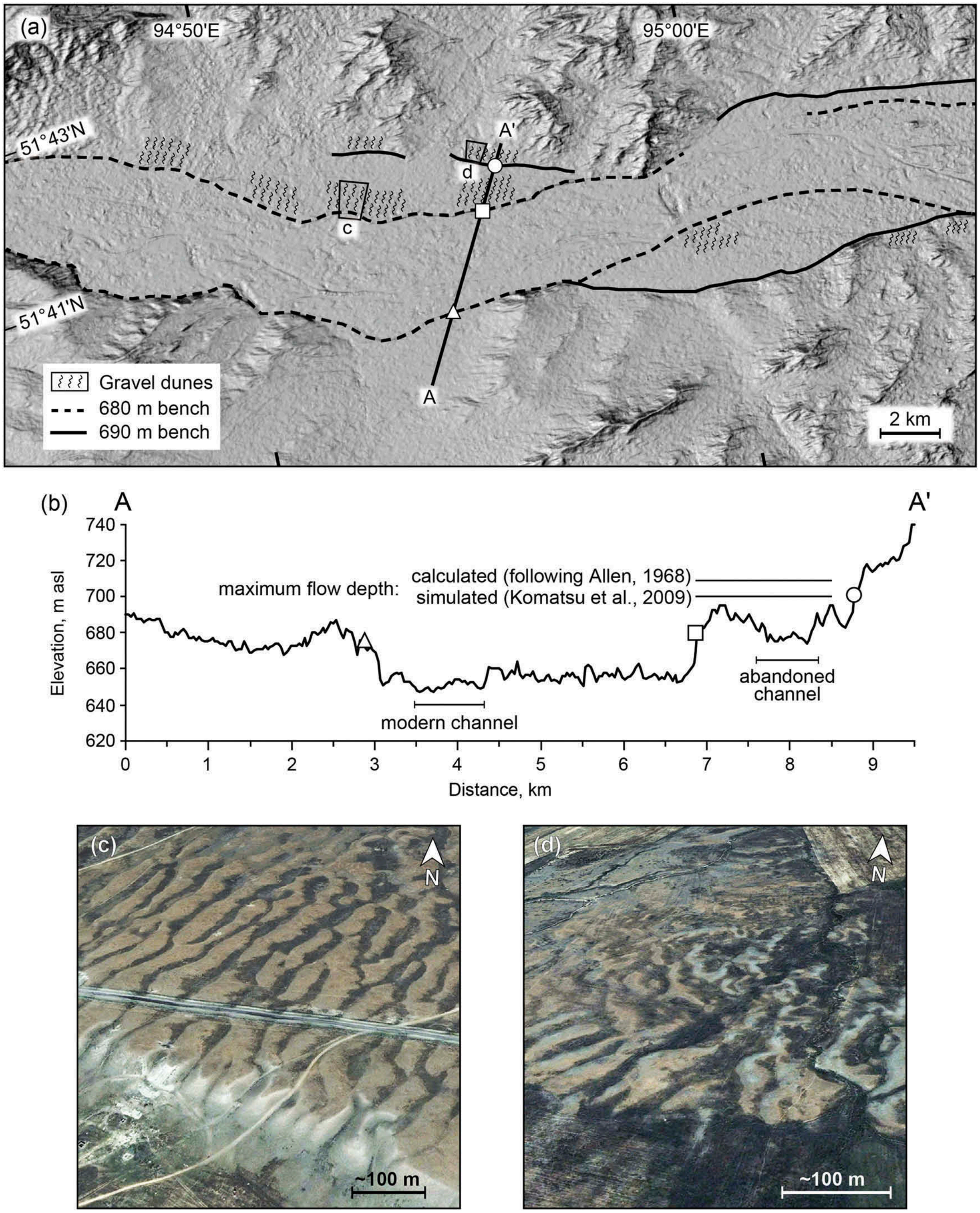

Figure 5. Giant gravel dunes in the Kyzyl basin. (a) Shaded-relief image from 15 m ASTER elevation data. Highest benches with gravel dunes are found up to 700 m asl. Lower but better-preserved gravel dunes are found at ~680 m asl. (b) Elevation profile along transect A–A′. Abandoned channels are present on the 680 m bench on both sides of the Maly Yenisei. The maximum depth of floodwater over the 680 m bench (~20 m) was estimated by Komatsu *et al*. (2009) using a numerical model. The 690 m bench continues up to 700 m asl, and the dune height of ~2 m is related to a flow depth of ~14 m using an equation of Allen (1968). The modern channel is at ~650 m asl. (c) Google Earth perspective view of the gravel dunes on the 680 m bench. (d) Google Earth perspective view of the gravel dunes on the 690 m bench. (Image data: DigitalGlobe.)

Grosswald (1987) was the first to attribute them to cataclysmic floods.

According to field observations by Komatsu *et al*. (2009) the gravel dunes are dune-shaped and asymmetrical, and the crests are nominally perpendicular to the river. The crest spacing is typically 50–80 m, and the amplitudes are a few metres. The dunes are rich in gravel, containing occasional boulders up to ~1 m in diameter. A top layer of loess overlies the cryoturbated gravels. Many of the gravel dunes occur in the lee of structural obstructions, such as bedrock knobs that would have slowed the floodwaters and reduced their carrying capacity for suspended sediment.

The Yenisei gravel dunes have smaller amplitudes and lower maximum wavelengths than those of the ones accumulated by the Altai floods down the Ob river from the Kuray–Chuya basins, some of which are 10 m or more in height and 100 m or more crest-to-crest. It is possible that the depths of the Yenisei floods were less than those of the Ob (cf. Wiedmer *et al*. 2010). Komatsu *et al*. (2009) suggested three other possibilities: (1) erosion of the dune crests after the flood events; (2) a limited supply of sediment to grow the dunes; and (3) scouring of the dunes by relatively calm floodwaters after the initially powerful floods.

Komatsu *et al*. (2009) estimated the stream power required for the dune formation to be 9–27 × 10^3 W m^{-2}, based on the empirical relationship between the stream power and cord length in the Channeled Scabland of Washington State, USA (Baker 1982). Because the dunes formed in the lee of obstructions, the stream power for the unimpeded floodwaters may have been greater than this estimated range; however, the estimated range is much lower than the values of 2×10^5 W m^{-2} estimated by O'Connor and Baker (1992) for the Missoula floods and 1×10^6 W m^{-2} by Baker *et al*. (1993) for the Altai floods.

Computer simulation of a flood from a 172 m-deep lake originating from Darhad basin (Komatsu *et al*. 2009) showed that the flow depth was ~20 m above the second-lowest terrace (water surface at 700 m asl). Using the empirical equation relating dune height and water depth by Allen (1968)[1] suggests that there were ~14 m of water above the highest gravel dunes at 700 m asl, consistent with numerical simulations by Komatsu *et al*. (2009). These gravel dunes could have been formed by multiple floods at different times, or by a single flood along the Maly Yenisei, in which the suspended loads were deposited at the highest level first and then at lower levels as the water flux decreased. A similar sequence of sedimentation at various levels from a single flood was observed in the Kuray and Chuya basins (Herget 2012).

2.2.2. The gorge of the Maly Yenisei in the East Sayan

Upstream of the Kyzyl basin, the Maly Yenisei flows for ~175 km through a deep (~0.5 km), narrow (~1.5 km), and roughly linear gorge that opens at its confluence with the Belin and Büsiin rivers (Figure 4). This double confluence is at the Mongolian border. The gorge continues east for another ~70 km to the confluence with the Tengis river, beyond which it broadens again at the entrance to Darhad basin. The river is typically 150 m wide near the Kyzyl basin, narrowing upstream to ~50 m. The underfit river meanders within the gorge.

Photo interpretation of satellite images shows that most of the tributaries to the Maly Yenisei in this reach lack large alluvial fans at their junctions, suggesting to Komatsu *et al*. (2009) that high-energy floods removed the pre-existing fans as well as incising the valley, as they suggested for the hanging valleys of the Ulug river.

Not all the flood deposits were eroded, however. On a big bend of the river, near (~18 km) the downstream end of the gorge (51.299750°N; 95.752750°E; 760 m asl), photo interpretation indicates multiple bars as much as 80 m above and on an inside bend of the river, a favourable location for deposition and preservation. In addition, other bar sequences are encountered ~15 km (51.343°N; 95.931°E) and ~35 km (51.334°N; 96.275°E) farther east, but still down river from the confluence of the Kyzyl and Kaa rivers. At the first site, bars are found on the north side of the gorge 16, 40, and 80 m above the modern Maly Yenisei. Across the river appears to be a barrier or cut-off bar, 90 m above the river and blocking a tributary canyon. At the second site bars are found 20, 40, 75, and 140 m above the river, again on the north side of the gorge. At (51.357°N; 96.867°E) an eroded veneer of sediment is found on the north side of the gorge up to 130 m above the river. All these bars are strong evidence for deep floods down the Maly Yenisei.

Near the confluence of the Kaa and Maly Yenisei rivers, basalt flows once filled the lower elevations of the gorge. The flows have been incised by the Maly Yenisei and today basalt flows (~100 m thick) cap terraces as much as ~250 m above the river. Although the gorge at the terrace elevation remains ~2 km wide, the steep-sided inner gorge through the flows here is only 0.9 km wide. Major tributaries have incised the flows, but lesser ones have not yet done so. Grosswald (1965) and Yarmolyuk *et al*. (2001) regarded the basalt flows as Pleistocene in age. In the Channeled Scabland, high-energy floods have deeply eroded hard basaltic rocks, both by abrasion and by plucking. Thus, Komatsu *et al*. (2009) suggested that the Maly Yenisei floods similarly contributed to the incision of the basalt terraces.

Grosswald and Rudoy (1996a, 1996b) went further and attributed the origin of the gorge itself to catastrophic floods. However, direct evidence for this has not been shown, and it seems likely that its early history – long before its flooding by the basalts – involved fluvial processes by the antecedent stream. Nevertheless, by analogy with the Channeled

Scabland, it seems possible that the incision of the inner gorge, cutting through the lava flows, could be due to catastrophic flooding.

Upstream from the basalt terraces and 8 km downstream from the confluence with the Belin (51.4892°N; 97.9941°E) there appears on satellite images to be at least one and possibly two steeply dipping strandlines (55 m km^{-1}) on the south side of the entrance to the ~1.5 km-wide gorge, 120 m above the river. Conceivably these resulted from the spillover from the hydraulic dam impounding Darhad floodwaters in the Büsiin–Belin valleys. Additionally, a possible run-up ramp is found immediately downstream in a steep tributary valley, also on the south side of the Maly Yenisei. Immediately upstream. Komatsu *et al*. (2009) calculated that 20 hours after the inception of a giant outburst flood from Darhad basin to the east, the water level behind the hydraulic dam would have reached a depth of ~247 m, although the calculated depths are uncertain because of the low resolution of the DEM available when the model was run (G. Komatsu, personal communication, 2015). If the floodwaters were impounded even to a depth of ~100 m, however, they would have reached ~30 km south along the Büsiin river and ~20 km north along the steeper Belin river. This temporary hydraulically dammed lake is shown in the modelled hydrographs of Komatsu *et al*. (2009), who calculated that it persisted for more than three days.

2.2.3. The Maly Yenisei from the Tuva border to Darhad basin

East of the border with Mongolia, the Maly Yenisei flows through a deep (1100 m), steep-sided (~30°) gorge in which few deposits appear to have been preserved. Here the glaciated peaks and ridges crowd closer to the river on both sides, and some moraines appear to lie only 80–90 m above the river (51.449990°N; 98.252850°E). The close approach of the palaeoglaciers may have been assisted by the steep slope, averaging 36° for the last 400 m above the Maly Yenisei; across the river to the north and in general, the end moraines appear to be ~350 m higher. The lowest termini of the glaciers may have been under water during the largest floods from Darhad basin: Komatsu *et al*. (2009) calculated that the flood depth 20 hours after the dam breached would have been ~130 m, such that the glaciers must have re-advanced after the last of the giant floods, as the moraines do not appear to have been eroded.

The broad (~15 km) Büsiin basin that straddles the border is a tectonic depression that was not filled with glacial ice during the Late Pleistocene, although it hosted a few large piedmont glaciers that were fed from the east (Ulaan Taiga). The tectonic basin continues north across the Maly Yenisei, where it is occupied by the Belin river. Although the upper Belin valley, above ~1200 m asl, hosted an outlet glacier from the East Sayan ice field (Grosswald 1965; Olyunin 1965; Arzhannikov *et al*. 2012), the lower valley was unglaciated. Nevertheless, its steep eastern wall – possibly a fault-line scarp – is marked by hanging valleys 250–300 m above the Belin river that resemble the hanging valleys along the Ulug river. We speculate from the resemblance that this wall was possibly eroded by outburst floods from the East Sayan ice field; these floods would have added further to the complexity of the flood record west of the border.

Between the international border and the Tengis river, near Darhad basin, the Maly Yenisei is flanked by sequences of terraces and bars (Komatsu *et al*. 2009; Figure 6a). The Tengis river was the site of the outlet glacier from the East Sayan ice field thought to have dammed palaeolake Darhad (e.g. Krivonogov *et al*. 2005). Near the western end of this reach, at (51.4622° N; 98.5786°E), the floor of the river valley is covered with kettle-pocked fill, 20 m above the modern river, probably due to a resurgent glacier entering the valley from the north. This till (?) is found at the same elevation both upstream 1 km and downstream 5 km. A glacier blocking the Maly Yenisei at 51.461°N and 98.574°E ('ice dam #4' in Komatsu *et al*. 2009) would impound the trunk river, but from the elevation of the uneroded moraine remnants it appears that the lake would back up only to about the confluence with the Tengis river and consequent flooding downstream would have been relatively minor.

At the downstream end of the putative till, photo interpretation suggests that a remarkable series of four arcuate bars fills a canyon mouth (51.444°N; 98.523°E). The elevation of the bars rises into the side canyon, from ~1465 to 1520 m asl; the convex sides point into the canyon also. The tributary valley is filled (to ~1510 m asl) with a flat deposit ~10 m lower than the impounding bars. Because they rise and point into the tributary, in this setting it seems unlikely that they could be glacial, and they may therefore represent a standing back-wave of one of the megafloods, up to 140 m above the modern channel.

For ~7 km upriver from the location of 'ice dam #4' (Figure 7) the Maly Yenisei flows through a V-shaped gorge that is straight, narrow (~2500 m) and deep (~800 m or more). The floor contains neither terraces nor large gravel bars. This gorge separates the Hoit Aguy massif from the Ulaan Taiga mountains.

Gillespie *et al*. (2008) suggested that the tributary Hadar Üüs valley on the eastern side of the Hoit Aguy

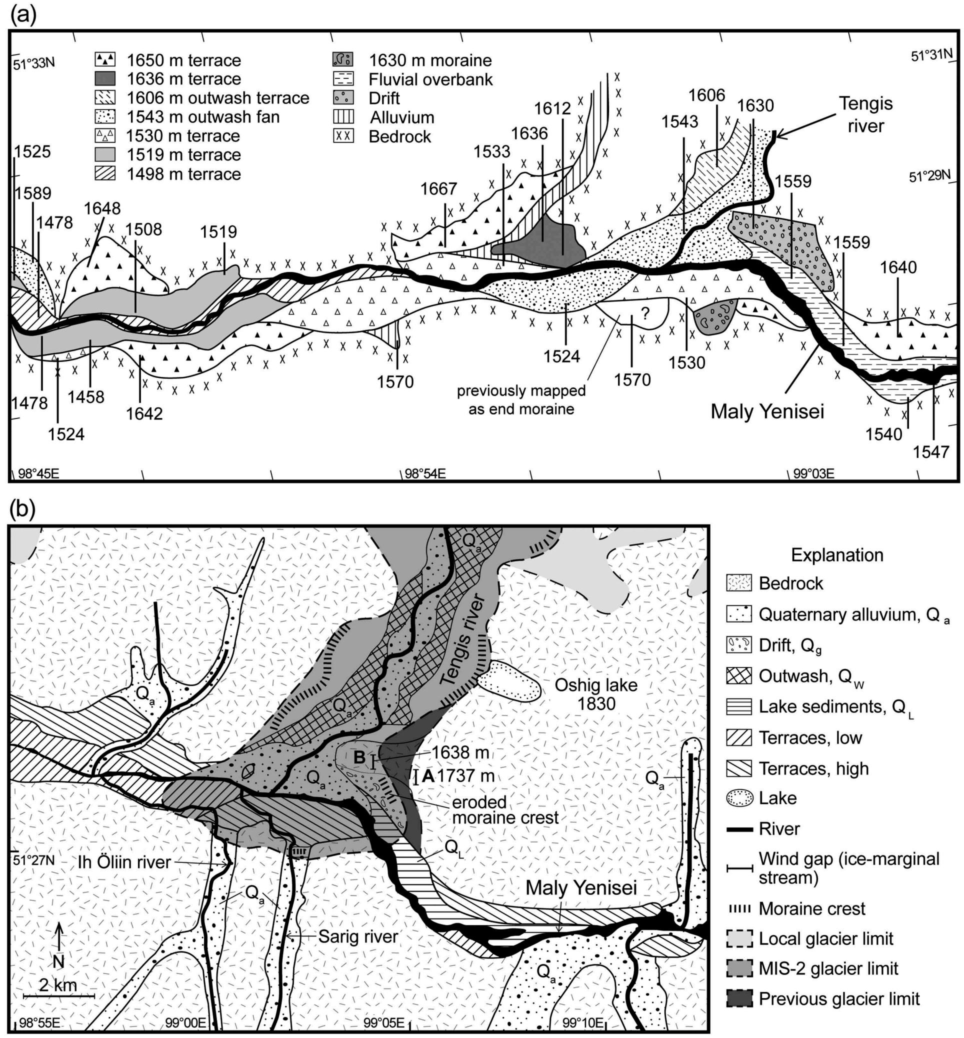

Figure 6. Maps of the lower Tengis river and the Maly Yenisei below the confluence showing: (a) Terraces with spot elevations from the SRTM. The sediments at the mouth of the Ih Öliin river valley at 1570 m asl do not appear to be in a moraine. The terminal moraine of the Tengis glacier sits in the mouth of the Sarig river valley at ~1630 m asl. Map adapted from Komatsu *et al*. (2009); (b) Extent of the late Pleistocene glaciers and deposits, adapted from Gillespie *et al*. (2008).

massif hosted an outlet glacier from the East Sayan ice field that likely dammed the Maly Yenisei ('ice dam #2': Figure 7). Here the lateral moraines and trimlines of the Hadar Üüs approach the Maly Yenisei closely. Ice dam #2 probably formed more than once. One possible moraine is at an elevation of ~1750 m asl, and in the absence of other dams upstream would have backed up a deep lake into Darhad basin. However, photo interpretation hints at an even higher, eroded moraine preserved at 1859 m asl ~1.6 km north of the Maly Yenisei. The glacier that built this moraine could in principle have impounded an even deeper lake. The interpretations are photo interpretive only (Google Earth), and no geological studies appear to have been made of this drainage and its ancient glaciers.

The Hoit Aguy massif itself was heavily glaciated, evident from the well-developed cirques, and wide, long side canyons with paternoster lakes. The end moraines limiting the paternoster lakes of the Hoit Aguy massif are found at 2050–2220 m asl, higher than the trimlines of the East Sayan outlet glaciers, suggesting that the local alpine glaciers did not dam the Maly Yenisei.

Upstream from the Hoit Aguy massif, the valley widens to ~3000 m and becomes flat-floored, with sets of terraces at 1498–1650 m asl, no higher than ~150 m above the river level (Figure 6a). The terraced floor extends ~22 km to the confluence with the Tengis river. Komatsu *et al*. (2009) described some of these terraces as having river-parallel (E–W) channels and levees, an indication of large floods. The highest are eroded intra-canyon basalt flows (e.g. Krivonogov *et al*. 2005), as was also the case in Tuva. At least some of these are capped by fluvial gravels (Komatsu *et al*. 2009).

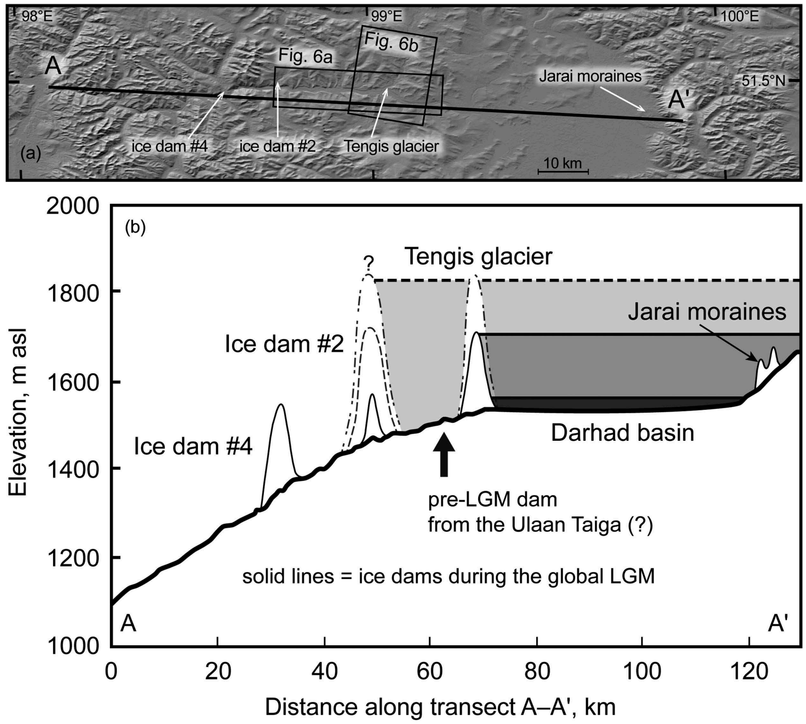

Figure 7. Topographic profile along the Maly Yenisei and across Darhad basin. (a) Locations indicated on the shaded-relief image from ASTER DEM. (b) Profile up the Maly Yenisei showing palaeo-highstands of Darhad basin and other glacier dams downriver. The 1825 m highstand (dashed line) exceeded the height of the Tengis moraines by ~100 m and likely predated MIS 2. Komatsu *et al*. (2009) hypothesized that an ice cap from the Ulaan Taiga mountains impounded the deepest palaeolake. We propose an additional blocking mechanism from the outlet glaciers of the East Sayan ice field, damming the Maly Yenisei near the Hoit Aguy massif.

Six kilometres west of the Tengis confluence, a pre-LGM ice cap in the Ulaan Taiga south of the Maly Yenisei may have sent ice into the gorge to block it (Komatsu *et al*. 2009). However, there is no direct evidence of the dam, located somewhere between ice dam #2 and the Tengis glacier dam, nor of its age.

The geomorphic evidence for the extent of the pre-LGM Ulaan Taiga ice cap is a set of eroded stepped bedrock terraces that once rose above it as nunataks. The lowest terraces are preserved above ~1950 m asl, on the edge of the valley and ~450 m above the modern Maly Yenisei. The top of a smaller, higher and younger ice cap is marked by fresh-appearing stepped terraces in Landsat images (Google Earth Pro ver. 7.1.2.2041 2015). This higher ice cap likely dates from MIS 2, the ^{10}Be age determined by Gillespie *et al*. (2008) for the terminal moraine of the Högiin outlet glacier from the Ulaan Taiga ice cap. An eroded lateral moraine remnant from the same valley dated >100 ka indicates the presence of an earlier ice cap also. No evidence suggests that the LGM Ulaan Taiga ice cap dammed the Maly Yenisei, but if the putative pre-LGM ice cap did so, it might have been responsible for the deepest palaeolake Darhad (1825 m asl).

Grosswald (1987, 1999) and Grosswald and Rudoy (1996b) earlier proposed an ice field spanning the Maly Yenisei and flowing together from both north (Sayan) and south (Ulaan Taiga). However, there is no evidence that the East Sayan ice field itself (except for the outlet glaciers) ever approached the Maly Yenisei closely, and their suggestion does not seem to have been widely accepted.

Krivonogov *et al*. (2005) and Komatsu *et al*. (2009) both identified what Krivonogov *et al*. called a 'fan terrace' about 50 m above the Tengis river. Komatsu *et al*. (2009) mapped this outwash surface west of the Tengis river at an elevation of 1606 m asl (Figure 6). This surface slopes down to the south at ~9 m km^{-1}. The outwash consists of sandy silts mixed with angular gravels underlying ~20 cm-thick dark soil. The modern Tengis river incises a lower outwash or alluvial fan (gravel and boulder 'cone' of Krivonogov *et al*. 2005) having a lower gradient (~7 m km^{-1}). They inferred that the upper terrace could have formed a dam reaching a minimum elevation of ~1580 m asl, and impounding a lake in Darhad basin to similar level. The incised lower fan terminates at two levels, 6 and 2 m above the modern Maly Yenisei according to Krivonogov *et al*. (2005). They suggested that these alluvial deposits may have impounded shallow lakes in Darhad basin. The fan must have originated after the Tengis had incised the 1606 m asl outwash plain, and its base level was 10 m or less above the modern Maly Yenisei. Furthermore, within ~0.5 km of the Maly Yenisei, the fan is approximately flat and does not grade up-river with the Tengis, although farther from the Maly Yenisei it does. The near-flat lower part of the fan may have been the spillway for the Maly Yenisei exiting the low palaeolake.

We observed in the field that for ~2 km east of the Tengis confluence the lower part of the fan, below ~1555 m asl, is covered with gravel dunes, ~1 m high and ~50 m crest-to-crest. They are perpendicular to the Maly Yenisei but oblique to the Tengis. These dunes likely formed due to currents of water draining the sediment-dammed lake and the flow was likely no deeper than 20–25 m, as calculated by the equation of Allen (1968). We infer that the dunes were formed during the last flood from a palaeolake with a surface level at ~1565 m asl, assuming that any later floods would have eroded them.

Upriver from the Tengis confluence, terraces still flank the Maly Yenisei on both sides, although their character is different. These terraces contain evidence of strong flow within one of the palaeolakes, such as might have followed the catastrophic breakup of the Tengis glacial dam. South of the river, one terrace at ~1560 m asl appears to be composed of or covered with light-toned lake sediments, such as are not observed downriver from the Tengis river. On the north side of the Maly Yenisei is a prominent terrace at ~1640 m asl (Figure 6) capped by sediments including bouldery granitic gravels and rounded basalt boulders up to 1 m in diameter. The basalt boulders appear to have been transported 1 km or so from their source (Komatsu *et al*. 2009). They are found in a region that is 100 m above the modern river but would have been under the Pleistocene highstands. The most likely mechanism for their transport would have been rapid draining of a Darhad palaeolake through Tengis dam ~9 km downstream. For 12 km upstream of Tengis dam the palaeolake would have been constricted to a canyon ~2.5 km wide, just as below the dam.

Fast flow is to be expected behind breached dams in rapidly draining lakes. Smith (2006) presented geologic evidence of strong flow in Lake Missoula after its ice dam was breached, and Bohorquez *et al*. (in this issue) modelled flow within the Kuray-Chuya palaeolakes, calculating flow speeds of ~18 to ~45 m s^{-1} there. These speeds are sufficient to move boulders as bedload. We can use the hydrographic models of Komatsu *et al*. (2009) to estimate a rough flow speed upstream from the breached Tengis dam that is in the lower part of the range from Kuray-Chuya. Within this reach the discharge of the floodwaters from palaeolake Darhad would have been spatially constant with an implied maximum flow speed of ~14 m s^{-1} at the breach to ~8 m s^{-1} near the boulders, where the water depth would have been greater. The bed shear stress of this flow is calculated to be enough to transport 1 m boulders (see details in online supplementary material). We conclude that currents within the draining palaeolake were strong enough near its outlet to cause erosion and transport of coarse bedload.

2.2.4. Evidence of a glacier dam at the Tengis river confluence

The early history of ideas concerning the impounding of palaeolakes in Darhad basin is well summarized by Krivonogov *et al*. (2005). The intra-canyon basalt flows must have blocked the Maly Yenisei at times, but the youngest of these basalt flows is ~6 million years old (Rasskazov *et al*. 2003; Ivanov *et al*. 2015). In this tectonically active region, it would be hard to reconstruct the highstand of any lakes dammed by the ancient lava flows. It is also possible that landslides have occasionally blocked the Maly Yenisei (e.g. Komatsu *et al*. 2009), but there is no direct evidence of this near the Tengis confluence in late Quaternary time. It appears that the Tengis glacier (Figure 4) is the main candidate for damming the Late Pleistocene palaeolakes that left most of the geomorphic evidence in the basin and the gorges of the Maly Yenisei although, as mentioned in the previous section, glacier dams farther downstream may have contributed also.

The moraine remnants of the glacier dams are sparse along the Maly Yenisei. Due to their location, they were eroded during large outburst floods. Furthermore, it is unclear how much debris was transported by the Tengis glacier to its terminus. If the glaciers were largely cold-based during the time leading up to the flood, they may well have transported little debris then, even if they became warm-based and relatively debris rich at the end of the glaciation as the climate warmed. We are thus left to look for moraine remnants away from the spillway floods.

Lateral moraines are preserved on the slopes of the Tengis river valley and are indirect evidence of the presence of a glacier dam across the Maly Yenisei. The right-lateral moraine 170 m above the modern Tengis river approaches the Maly Yenisei to within ~2 km. The glacier that left this moraine would likely have impounded a palaeolake in Darhad basin to a level of ~1710 m asl.

A higher left-lateral Tengis moraines is found at ~1840 m asl, impounding the Oshig lake (Figure 6b). The glacier that left this moraine must have been >270 m deep. Although the moraines at Oshig lake are preserved no closer than ~5 km from the Maly Yenisei, both Krivonogov *et al*. (2005) and Gillespie *et al*. (2008) observed exotic clasts on the ridge between the Tengis and Maly Yenisei valleys at 1831 and ~1825 m asl, respectively, and considered them to have been glacially transported. The glacier may have impounded a palaeolake in Darhad basin to a level of ~1825 m asl.

Merle (2001), Krivonogov *et al*. (2005), and Gillespie *et al*. (2008) all reported remnants of end moraines blocking the mouths of two neighbouring valleys across the Maly Yenisei from the Tengis river (Figure 6b). We have now visited the eastern of these valleys (Sarig river) and confirm that the ridge there is indeed a moraine, with its crest at ~1630 m asl. It is covered with exotic porphyritic granite boulders up to 3 m in diameter. The other sediment ridge near the mouth of the Ih Öliin river (Figure 6b) is much lower (1570 m asl) than the end moraine in the Sarig valley. If this mound was an end moraine, the floodwater must have eroded its top. We propose two alternative hypotheses for its formation: it could be a barrier bar that was deposited by an energetic flood, or it could be the runout from a landslide from the western wall of the valley. Krivonogov *et al*. (2005) mapped it as an 'ice-push scarp' from the Tengis glacier. A second fresh landslide scar is found adjacent to the first, but on the southern wall of the Maly Yenisei valley. The runout from this second landslide is nowhere to be found; perhaps it was eroded by the outburst floods. In their Figure 3a, Krivonogov *et al*. (2005) mapped their 'end moraine' as a low (~10 m according to Google Earth) approximately circular feature ~0.5 m in diameter and 1 km south of the 'barrier bar'. This putative moraine remnant lacks an associated headwall scarp and therefore lacks critical evidence that would identify it as a landslide, too. There appears to have been no detailed field study of these important geomorphic features.

There are two N–S-oriented bedrock wind gaps on the mountain ridge separating the Tengis and Maly Yenisei valleys today. The eastern, higher wind gap (A: Figure 6b) is ~10 m deep where it crosses the ridge at ~1737 m asl; the incision terminates on the north side of the ridge at ~1725 m asl, but on the south side it terminates at ~1695 m asl. This asymmetry suggests water once flowed south out of Tengis valley through the wind gap >160 m above the modern Tengis river. The source of the temporary river was likely an ice-marginal lake impounded by one of the Tengis glaciers. The flow appears to have been into a palaeolake with a surface ~45 m or more below the spillway and ~145 m above the modern Maly Yenisei.

The western, lower wind gap (B: Figure 6b) likely had a similar origin and history. It is eroded into basalt at ~1638 m asl. Gillespie *et al*. (2008) found ~2 m granodiorite boulders, originating from the Tengis headwaters, sitting atop the water-eroded basalt in the spillway. Transportation of the exotic boulders to the vicinity of the lower wind gap must have been via the Tengis glacier, but through the narrow wind gap the most likely mechanism was an ice-marginal river flowing rapidly (several m s^{-1}) into a lower and more recent Darhad palaeolake than the one into which the upper wind gap drained. These boulders in the lower wind gap yielded ^{10}Be ages of 21 and 24 ka (Gillespie *et al*. 2008).

Above we mentioned the suggestion of Krivonogov *et al*. (2005) that post-glacial sediments may have dammed the Maly Yenisei. Kettle topography and the large volume of sediments flanking the Tengis river (~8 km^3) suggested to Gillespie *et al*. (2008) that a debris-rich glacier in the Tengis valley persisted for some time after its initial retreat. This could have been the case even if the glacier at its maximum advance was cold-based and debris-poor.

2.2.5. Evidence of a palaeolake in Darhad basin

Darhad basin is ~100 km long (north–south) and 20–40 km wide. The clearest evidence of deep palaeolakes in Darhad basin is the presence of shorelines (Selivanov 1967) on the walls east of the Tengis river at 1593 to 1713 m asl, the latter equivalent to a palaeolake with a surface 172 m above the modern level of Lake Dood Tsagaan (Figures 7, 8). Gillespie *et al*. (2008) observed higher shorelines indicated by degraded horizontal terraces on the basin walls near Zayadai lake as high as 1825 m asl. Krivonogov *et al*. (2005) measured the elevations of 47 shorelines near the Tengis valley, although most could not be followed around the basin. They considered the shorelines up to 1713 m asl to represent temporary stillstands of the rising lake that were not eroded during the subsequent rapid drawdown. The higher shoreline must have been left by an older, deeper lake.

Not all the lake-shore features are horizontal. A notch in the northern wall of the pass connecting Zayadai lake (Figure 8) to the main Darhad basin slopes to the east, at 3–4 degrees, suggesting strong outflow through the narrow pass to a lower lake in the main basin. The gradient could have resulted from either an outburst flood from the headwaters of the Shishhid river in the Ulaan Taiga, filling the Zayadai sub-basin first, or from rapid lowering of the lake in the main basin during an

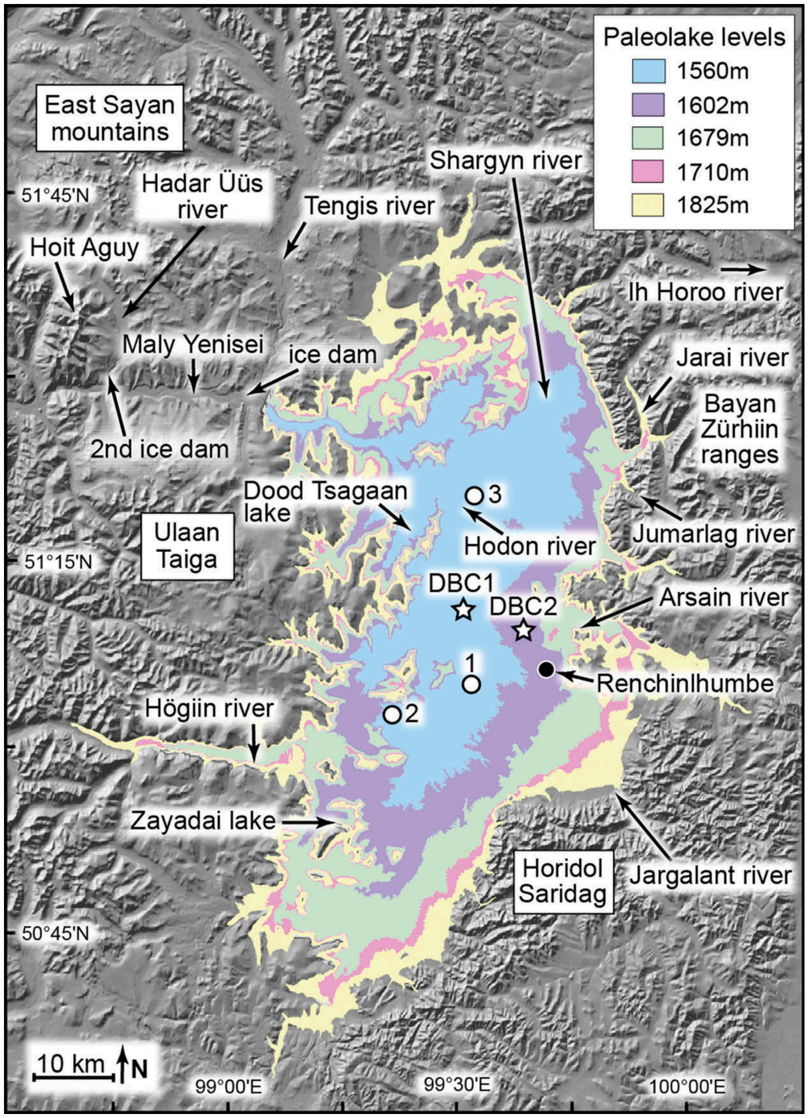

Figure 8. Geographic names and the extent of the palaeolake when Darhad basin filled to 1560, 1602, 1679, 1710, and 1825 m asl. Circles numbered 1, 2 indicate wells of Ufland *et al.* (1971), and 3 indicates DDB10-3 core (Krivonogov *et al.* 2012). Star symbols indicate two wells of Gillespie *et al.* (2005). Shaded-relief image from SRTM data. The map is from Gillespie *et al.* (2008).

outburst flood down the Maly Yenisei. Prominent highstands of palaeolake Darhad and their corresponding parameters are summarized in Table 4.

Near the town of Renchinlhumbe, aeolian sand streaks up to a ~1.5 km-long point southeast, probably reworked from lacustrine and fluvial sands. These are

Table 4. Highstands and volumes of the palaeolake Darhad.

Highstand elevation (m asl)	Lake volume (km^3)	Location of the highstand
1825	809	Degraded shorelines near Zayadai lake[a] Exotic clasts transported by the Tengis glacier[a, b] Trimlines of outlet glaciers from the East Sayan ice field (Hoit Aguy) Left-lateral moraine of the Tengis impounding Oshig lake[a]
1710	373	Beach sands 2 km south of Jarai river, near the Jumarlag river[a] Wind gap (1732 m asl) east of the Tengis river[a]
1679	276	Highest shoreline cut on the MIS 2 Jarai moraines[a]
1602	85	Outwash plain west of the Tengis river, measured near erosional scarp ~11 cal ka BP clam shells from a shoreline near Zayadai lake[a] 10–11 cal ka BP larch twigs in lake sediments near Jarai river[a]
1560	16	Outwash from Jargalant or Arsain rivers, terminating ~13 km south of Arsain river[a]

[a]The evidence and data from Gillespie *et al.* (2008).
[b]Krivonogov *et al.* (2005) measured the elevation up to 1831 m asl.

readily visible on Google Earth and must postdate the final draining of the palaeolakes. There are also fluvial dune fields. Two such fields that we have visited are downstream from where rivers empty into the basin. The geographic coincidence suggests that these may be related to floods draining into the basin, rather than from floods originating in the basin itself. At Högiin river (Figure 8), the dunes may have been left by outburst floods when an impounded lake breached its moraine dam there (Carson *et al*. 2003). West of the Renchinlhumbe, gravels up to 15 cm in diameter overlie the lake sediments. They are shallowly buried below 1578 m asl and must have been deposited as a fan or delta of the Jargalant or Arsain rivers after the last of the deep palaeolakes drained.

Lake sediments in Darhad basin are rich in fossils of comparatively deep-water biota, such as clam and ostracod shells, fish scales, and aquatic plants. The dated fossils from the cutbanks of the Shargyn river indicate a lake existed during MIS 3 (Gillespie *et al*. 2008) for enough time to establish large populations (Gravis 1974). In addition to aquatic biota there are many subaerial plant fossils (e.g. larch twigs, moss, and other terrestrial plants) found in the lake sediments indicating that the Darhad palaeolake level fluctuated, and sometimes the basin was mostly dry (Gillespie *et al*. 2008).

2.2.6. Permafrost in Darhad basin

Shallow permafrost cannot persist beneath long-standing lakes, so permafrost in Darhad basin must either date from the Holocene, after the basin was largely drained, or the palaeolakes must have been short-lived, or both. Today, the floor of Darhad basin has shallow ground ice, many thermokarst lakes, ice wedges, and other evidence of permafrost. Sharkhuu *et al*. (2007) estimated that the active layer near Dood Tsagaan lake reaches 1.5 m, and attributed its shallow depth to the low thermal conductivity of ice-rich, fine-grained sediments.

Gravis (1974) considered the permafrost in Darhad basin to have formed at the end of the MIS 2 Sartan glaciation, but Krivonogov *et al*. (2005) related the existence of MIS 2 permafrost in the Mongolian Gobi (Owen *et al*. 1998) to the formation age for the ice wedges and frost-heaved mounds in Darhad basin, and suggested that the basin was largely dry during MIS 2. Therefore, there could have been no deep persistent palaeolake from MIS 2. Later, Krivonogov *et al*. (2012) dated disseminated plant materials in the fill sediments of a thermokarst depression near Shargyn river to ~8.1 cal ka BP, suggesting to them that the modern permafrost in Darhad basin formed since then, in agreement with Gravis (1974). Krivonogov *et al*. (2012) also estimated that the permafrost in Darhad basin was thicker in the south (>127 m) than in the north (~47 m), based on the maximum depth of ground ice encountered in the deep boreholes of Ufland *et al*. (1971), Gillespie *et al*. (2005), and Krivonogov *et al*. (2012) (Figure 8). Equating the depth of the ground ice to its age, Krivonogov *et al*. (2012) inferred that Darhad basin started drying from the south.

These arguments and the absence of MIS 2 lake sediments at the Shargyn river cutbank are the basis of the contention that the latest deep palaeolake in Darhad basin, and the latest megafloods down the Maly Yenisei, dated from MIS 3 or earlier. On the other hand (section 3), ages for piedmont moraines around the basin are MIS 2 (Gillespie *et al*. 2008), suggesting that the Tengis glacier was large enough to have dammed the Maly Yenisei at least intermittently. These conflicting conclusions are at the heart of the controversy identified by Krivonogov *et al*. (2012).

2.2.7. Summary of the flood and palaeolake evidence

The past existence of a large lake in Darhad basin is evident from shoreline features and abundant lacustrine sediments. Subaerial plant fossils found in the Shargyn cutbanks show that the palaeolakes were drained or partially filled the basin at some time. The large-scale angular unconformities visible in the cutbanks suggest erosion of sediments during the outburst floods. A glacial dam is the most viable mechanism to create such deep and ephemeral lakes. However, sediment dams at Tengis river, such as from the alluvial fans or outwash terraces, likely formed shallower lakes following the major glacial retreats. Hanging valleys and strath terraces in the valley of the Maly Yenisei are attributed to the outburst floods of the palaeolake Darhad (section 2 above). Floodwaters deposited large amount of sediment downstream as large gravel dunes and fluvial terraces in the Kyzyl basin. However, none of these flood deposits downstream from Darhad basin have been directly dated so far and the only constraint on timing of these flood events themselves is indirect, from the dating of glacial deposits around Darhad basin and adjacent areas, but not from the deposits associated with the putative glacial dam itself.

Although long sediment cores (~140 m) have been extracted from the centre of Darhad basin (Ufland *et al*. 1971), these have no associated age control. Recent shallow-water sediments have been dated near the depocentre of Darhad basin, but deep-lake sediments have only been dated near the shores, where erosion, slumping, and the potential for an incomplete record is greatest (e.g. Shargyn cutbank section of Gillespie *et al*. 2008, maximum water depth ~155 m). An age model for the deep-water sediments from the largest palaeolakes that generated the biggest floods down the Maly Yenisei has not been generated.

3. Timing of the floods

Without direct dating of the eroded Tengis dam remnants and the flood sediments downriver, the timing of the Maly Yenisei flood events has been constrained only indirectly, by dating lake sediments and glacial deposits in and around Darhad basin. In this section we review previous dating efforts for such purposes.

3.1. Quantitative dating of lake sediments in Darhad basin

A pair of ^{14}C ages for bulk sediments and a wood sample retrieved from below the modern floor of the Dood Tsagaan lake showed that the bulk sediments appeared to be ~3500 ^{14}C years older than the wood (Peck *et al*. 2001). The discrepancy was attributed either to hard-water effects or to the influx of older detrital sediments to the lake bottom. Gillespie *et al*. (2008) recommended correcting the ^{14}C ages of shells by 2500 ^{14}C years, based on the age discrepancy between a pair of larch twigs and snail shells sampled from the same depth in the lake sediments overlying the Jarai outwash. A similar experiment was performed at the Hodon river cutbank by Krivonogov *et al*. (2012); their ^{14}C ages for shells of molluscs consistently overestimated the ages for wood by ~2500 ^{14}C years. The molluscs were filter feeders and detritivore species, and their probable intake of old carbon was attributed to the age discrepancy. We applied the correction of 2500 ^{14}C years to the published ages for shells and bulk sediments. Gillespie *et al*. (2008) treated the peat samples as bulk organics and we applied a 2500 ^{14}C years correction to the recalibrated ages. If individual fragments of plants, including larch twigs, roots, and grasses, were extracted from the peat or bulk sediments the correction was not applied to those macrofossil ages. Hereafter, only the recalibrated and corrected published ^{14}C ages, summarized in Table 5, are referred to in this review.

^{14}C dating was first used on sediments extracted from the modern Dood Tsagaan lake (Figure 8) by Dorofeyuk and Tarasov (1998). Their gyttja samples at depths of 1.2 and 2.4 m below the lake floor, respectively, yielded ages of ~6.6 and ~10.8 cal ka BP after correction. The deepest part of Dood Tsagaan lake was cored by Peck *et al*. (2001), and the surface bulk sediments yielded corrected ^{14}C ages of ~0.4 cal ka BP. At a depth of ~4 m in the core, the age for bulk sediments was ~6.4 cal ka BP corrected to ~2.9 cal ka BP, which is closer to the age for a wood sample of ~2.1 cal ka BP from the same depth. Krivonogov *et al*. (2012) augmented the earlier studies in Darhad basin, extracting three short cores from the modern lake Dood Tsagaan. Eleven bulk organic samples taken at various depths from the 6.4 m core (DN-1) gave ^{14}C ages ranging from ~9.5 to 12.7 cal ka BP. A second core from Dood Tsagaan lake (DN-2: 4.3 m long) was studied by Narantsetseg *et al*. (2013), who reported ^{14}C ages of ~4.8 and ~5.1 cal ka BP for bulk organics from depths of 0.5 and 2.6 m, respectively, which appear to imply rapid sedimentation of ~7 mm year^{-1}. Krivonogov *et al*. (2012) reported a ^{14}C age of ~14 cal ka BP for wood found at a depth of ~4 m in the same core. If these ages are accurate it suggests a variable sedimentation at this site.

Gillespie *et al*. (2008) provided a more complete chronology of lake evolution and glacial advances in Darhad basin, using ^{14}C dating of organics, including twigs, incorporated in the lake sediments. They also used infrared-stimulated luminescence (IRSL) for directly dating the lake sediments, and CRE dating for the glacially abraded and transported boulders found on moraines. These are summarized below.

There are lake silts at 1581 m asl, overlying the outwash plain deposited by the palaeoglaciers of Jarai river valley. Peat, shells, charcoal, and wood were sampled from the same depth of ~1 m, and the consistent ^{14}C ages for the six samples gave an average age of ~10.1 cal ka BP. Two shell samples from ancient beach sands at 1602 m asl near Zayadai lake (Figure 8) dated to 10.3 and 11.2 cal ka BP. These ages suggest that Darhad palaeolake was at least 65 m deep in the early Holocene, consistent with the presence of a lower sediment (outwash) dam but not the higher ice dams at the Tengis confluence.

An outcrop at the Hodon river cutbank (Figure 8) exposes a ~13 m-thick section of lake sediments at 1552 m asl. Krivonogov *et al*. (2012) dated 16 samples taken from this cutbank, including four pairs of wood and shell from the same depths (3.6, 5.2, 5.6, and 7.0 m). The uppermost layer was dated to ~4.8 cal ka BP. The ages increased with depth, and the layer at ~10 m depth was dated to ~9 cal ka BP. Based on the sandy composition and abundance of wood materials at lower sections of the Hodon outcrop, Krivonogov *et al*. (2012) argued that Darhad basin was largely dry by ~9 ka. Narantsetseg *et al*. (2013) extracted diatom remnants in the sediments from the DN-1 and DN-2 cores, but did not find any diatom fossils in the sediments from ~10–14 ka. The minimal concentration of organic carbon coincided with the absence of diatoms in the palaeolake Dood Tsagaan, suggesting to

Table 5. ^{14}C samples collected in Darhad basin.

Sample ID	Lab number	Material	Depth (m)	^{14}C age (^{14}C year BP ± 1σ)	Calibrated age[a] (cal year BP ± 2σ)	Corrected ages for hard-water effect[b] (cal year BP ± 2σ)	References
Jarai river, lake silts overlying outwash below the end moraines: 51.400067°N, 99.751650°E, 1581 m asl							
100800 rmb-03	76360	Peat	1.12	11090 ± 60	12940 ± 140	10440 ± 140	Gillespie *et al.* (2008)
100800 rmb-03	76361	Wood from peat	1.12	5700 ± 50	6520 ± 120	6520 ± 120	
100800 arg-03	76694	Charcoal	1.00	9200 ± 40	10345 ± 95	10345 ± 95	
072301 arg-001a	79695	Wood	1.00	9480 ± 40	10695 ± 105	10695 ± 105	
072301 arg-001a	79696	Snail shells	1.00	11930 ± 40	13710 ± 140	11210 ± 140	
260701 rmb-10 #5	79698	Clam shells	1.00	11900 ± 40	13680 ± 110	11180 ± 110	
Zayadai lake, lacustrine silts underlying reworked beach sands: 50.900050°N, 99.229217°E, 1602 m asl							
071901 arg-002	79697	Clam shells	1.20	10960 ± 50	12845 ± 125	10345 ± 125	Gillespie *et al.* (2008)
071901 arg-003	79698	Snail shells	1.20	11810 ± 50	13650 ± 110	11150 ± 110	
Shargyn river cutbank in Jarai delta, lake silts: 51.401550°N, 99.750183°E, 1563 m asl							
062002 arg JG-04	97489	Charred wood	0.25	3285 ± 40	3525 ± 85	3525 ± 85	Gillespie *et al.* (2008)
062002 arg JG-04	97490	Wood charcoal	0.25	3210 ± 40	3435 ± 75	3435 ± 75	
062002 arg SG-n1	97491	Vegetation stems	1.85	47500 ± 1900	51495 ± 3025	51495 ± 3025	
062002 arg SG-n2	97492	Grass	2.10	47400 ± 1900	51355 ± 3015	51355 ± 3015	
062002 arg SG-n5	97493	Organic matter	2.54	45700 ± 1500	49230 ± 2330	49230 ± 2330	
062002 arg SG-n9	97494	Vegetation remains	3.23	46200 ± 1600	49810 ± 2540	49810 ± 2540	
062002 arg SG-n19	97495	Grass blades	7.13	49500 ± 2400	55350 ± 4700	55350 ± 4700	
062102 arg SG-n2-1	97496	Organic matter	2.72	51700 ± 3200	>50000	>50000	
062102 arg SG-n2-2	97497	Mat fibers	3.89	52800 ± 3600	>50000	>50000	
062102 arg SG-n2-7	97498	Moss fragments	7.84	48500 ± 2100	53075 ± 3395	53075 ± 3395	
260701 rmb-10 #7	79699	Fish scale	~8.40	39300 ± 2600	43280 ± 4970	43280 ± 4970	
260701 rmb-10 #3	79700	Wood twigs	~8.40	>modern	>modern	>modern	
260701 rmb-10 #1	79701	Wood fragments	~8.40	>35700	>41000	>41000	
260701 rmb-10	80308	Aquatic plants	~8.40	33600 ± 1500	37905 ± 3155	37905 ± 3155	
Tengis river confluence with Maly Yenisei river, lake silts: 51.440483°N, 99.061283°E, 1540 m asl							
180800 rjc	71885	Clam shells	1.00	10530 ± 40	12510 ± 110	10010 ± 110	Gillespie *et al.* (2008)
Tengis river outwash, interbedded silt: 51.650383°N, 99.118083°E, 1729 m asl							
150800 rmb-02	76362	Wood	0.90	7750 ± 40	8515 ± 85	8515 ± 85	Gillespie *et al.* (2008)
Högiin river moraine: 51.005767°N, 99.141450°E, 1716 m asl							
200800 rmb-02	76363	Wood	0.38	1060 ± 50	990 ± 90	990 ± 90	Gillespie *et al.* (2008)
DDP10-3 borehole: 51.336330°N, 99.501639°E, 1554 m asl							
-	ICa100044	Shells	8.02	7280 ± 60	8085 ± 115	5585 ± 115	Krivonogov *et al.* (2012)
Dood Tsagaan lake (central basin) DN-1 borehole: 51.407200°N, 99.325194°E, 1538 m asl, water depth 3.5 m							
-	AA79206	Roots of herbs	0.74	8500 ± 40	9500 ± 40	9500 ± 40	Krivonogov *et al.* (2012)
-	AA79207	Roots of herbs	1.87	10780 ± 60	12685 ± 85	12685 ± 85	
-	AA79208	Piece of stem	1.98	10730 ± 45	12665 ± 65	12665 ± 65	
-	AA79209	Shell (mollusk)	2.09	10870 ± 45	12750 ± 60	10250 ± 60	
-	AA79210	Plant fragment	2.21	10720 ± 45	12660 ± 70	12660 ± 70	
-	AA79212	Shell of pelecipod	2.95	11690 ± 60	13520 ± 120	11020 ± 120	
-	AA79213	Shells of Lymnaea	4.49	11270 ± 110	13095 ± 245	10595 ± 245	
-	AA79214	Charcoal	5.64	8690 ± 45	9660 ± 120	9660 ± 120	
-	AA79215	Pieces of wood	5.85	9590 ± 55	10945 ± 205	10945 ± 205	
-	AA79216	Pieces of wood	6.44	9810 ± 45	11230 ± 60	11230 ± 60	

(*Continued*)

Table 5. (Continued).

Sample ID	Lab number	Material	Depth (m)	^{14}C age (^{14}C year BP ± 1σ)	Calibrated age[a] (cal year BP ± 2σ)	Corrected ages for hard-water effect[b] (cal year BP ± 2σ)	References
Dood Tsagaan lake (central basin) DN-2 borehole: 51.395389°N, 99.359361°E, 1538 m asl, water depth 3.5 m							
-	AA94382	Bulk organics	0.56–0.58	6410 ± 50	7345 ± 75	4845 ± 75	Narantsetseg *et al.* (2013)
-	AA94383	Bulk organics	2.60–2.62	6780 ± 45	7630 ± 60	5130 ± 60	Narantsetseg *et al.* (2013)
-	AA79217	Pieces of wood	4.13	12130 ± 50	13980 ± 170	13980 ± 170	Krivonogov *et al.* (2012)
Hodon river cutbank: 51.335833°N, 99.500778°E, 1552 m asl							
-	ICa100033	Shells (mollusk)	0.55–0.6	6380 ± 50	7330 ± 90	4830 ± 90	Krivonogov *et al.* (2012)
-	ICa100034	Shells (mollusk)	2.20	6540 ± 60	7490 ± 80	4990 ± 80	
-	IWd100391	Wood	3.25	4920 ± 50	5670 ± 80	5670 ± 80	
-	ICa100035	Shells (mollusk)	3.25	6650 ± 50	7515 ± 75	5015 ± 75	
-	ICa100036	Shells (mollusk)	4.18	8350 ± 60	9360 ± 130	6860 ± 130	
-	ICa100037	Shells (mollusk)	4.85	8630 ± 60	9615 ± 125	7115 ± 125	
-	IWd100392	Wood	5.15	5180 ± 50	5940 ± 80	5940 ± 80	
-	ICa100038	Shells (mollusk)	5.15	8590 ± 60	9585 ± 105	7085 ± 105	
-	IWd100393	Wood	5.63	7420 ± 60	8270 ± 110	8270 ± 110	
-	ICa100039	Shells (mollusk)	5.63	9280 ± 60	10425 ± 165	7925 ± 165	
-	IWd100394	Wood	7.01	6970 ± 60	7785 ± 95	7785 ± 95	
-	ICa100040	Shells (mollusk)	7.01	9760 ± 70	11195 ± 125	8695 ± 125	
-	ICa100041	Shells (mollusk)	8.31	9870 ± 70	11300 ± 120	8800 ± 120	
-	ICa100042	Shells (mollusk)	8.91	10040 ± 70	11550 ± 280	9050 ± 280	
-	ICa100043	Shells (mollusk)	10.08	10130 ± 70	11715 ± 315	9215 ± 315	
-	IWd100395	Wood	10.80	7690 ± 60	8495 ± 95	8495 ± 95	
Talyn lake, palaeolake sediments: 51.4333°N, 99.6168°E, 1554 m asl							
-	IWd100396	Wood	2.50	55260 ± 2080	>55000	>55000	Krivonogov *et al.* (2012)
Shargyn river, filling of a thermokarst basin: 51.4167°N, 99.6167°E, 1543 m asl							
-	SOAN-5080	Plant fragments	3.85	7075 ± 75	7875 ± 145	7875 ± 145	Krivonogov *et al.* (2012)
-	SOAN-5081	Plant fragments	7.00	7255 ± 85	8075 ± 145	8075 ± 145	
Jumarlag river, filling of a thermokarst basin: 51.4000°N, 99.6667°E, ~1550 m asl							
-	Beta-174246	Wood	3.00	5140 ± 40	5905 ± 45	5905 ± 45	Krivonogov *et al.* (2012)
Jumarlag river, filling of a thermokarst basin: 51.3833°N, 99.6667°E, ~1550 m asl							
-	SOAN-5079	Wood	4.00	3180 ± 50	3415 ± 95	3415 ± 95	Krivonogov *et al.* (2012)
Tsagaan lake, thermokarst lake sediments: 51.3339°N, 99.5000°E, 1540 m asl							
-	SOAN-5532	Humic soil	1.20	3515 ± 75	3795 ± 185	3795 ± 185	Krivonogov *et al.* (2012)
Jarai river, sand cover above periglacial fan: 51.4000°N, E 99.7500°E, 1579 m asl							
-	SOAN-5531	Wood	1.00	2460 ± 25	2465 ± 85	2465 ± 85	Krivonogov *et al.* (2012)
DBC1 borehole: 51.187222°N, 99.497556°E, 1547 m asl							
-	AA-79019	Roots of herbs	16.27	15530 ± 140	18790 ± 300	18790 ± 300	Krivonogov *et al.* (2008)
Dood Tsagaan lake (southern basin): 51.3000°N, 99.3700°E, 1538 m asl, water depth ~14 m							
-	-	Bulk sediments	surface	3570 ± 36[c]	3900 ± 80	400 ± 80	Peck *et al.* (2001)
-	-	Bulk sediments	4.09	5530 ± 55[c]	6350 ± 90	2850 ± 90	
-	-	Wood	4.09	2080 ± 21[c]	2060 ± 60	2060 ± 60	
Dood Tsagaan lake (southern basin): 200 m from its eastern shore, 51.3333°N, 99.3833°E, 1538 m asl, water depth 3.3 m							
-	Vib-112	Gyttja	1.23	8150 ± 60	9140 ± 150	6640 ± 150	Dorofeyuk and Tarasov (1998)
-	Vib-113	Gyttja	2.38	11470 ± 100	13290 ± 190	10790 ± 190	

[a] 2σ range calculated using CALIB version 7.1 (Stuiver and Reimer 1993) and IntCal13 calibration curve (Reimer *et al.* 2013), and rounded to nearest decade.
[b] Hard-water corrections to the ages for bulk sediments, peat, and gyttja were taken from the recommendations of the corresponding articles.
Gillespie *et al.* (2008): 2500 14C year; Krivonogov *et al.* (2012): 2500 14C year; Peck *et al.* (2001): 3500 14C year; We used 2500 14C year for ages of Krivonogov *et al.* (2005), Krivonogov *et al.* (2008)) and Dorofeyuk and Tarasov (1998).
[c] Peck *et al.* (2001) did not provide the uncertainty, and we assumed 1% error, rounded to the nearest decade.

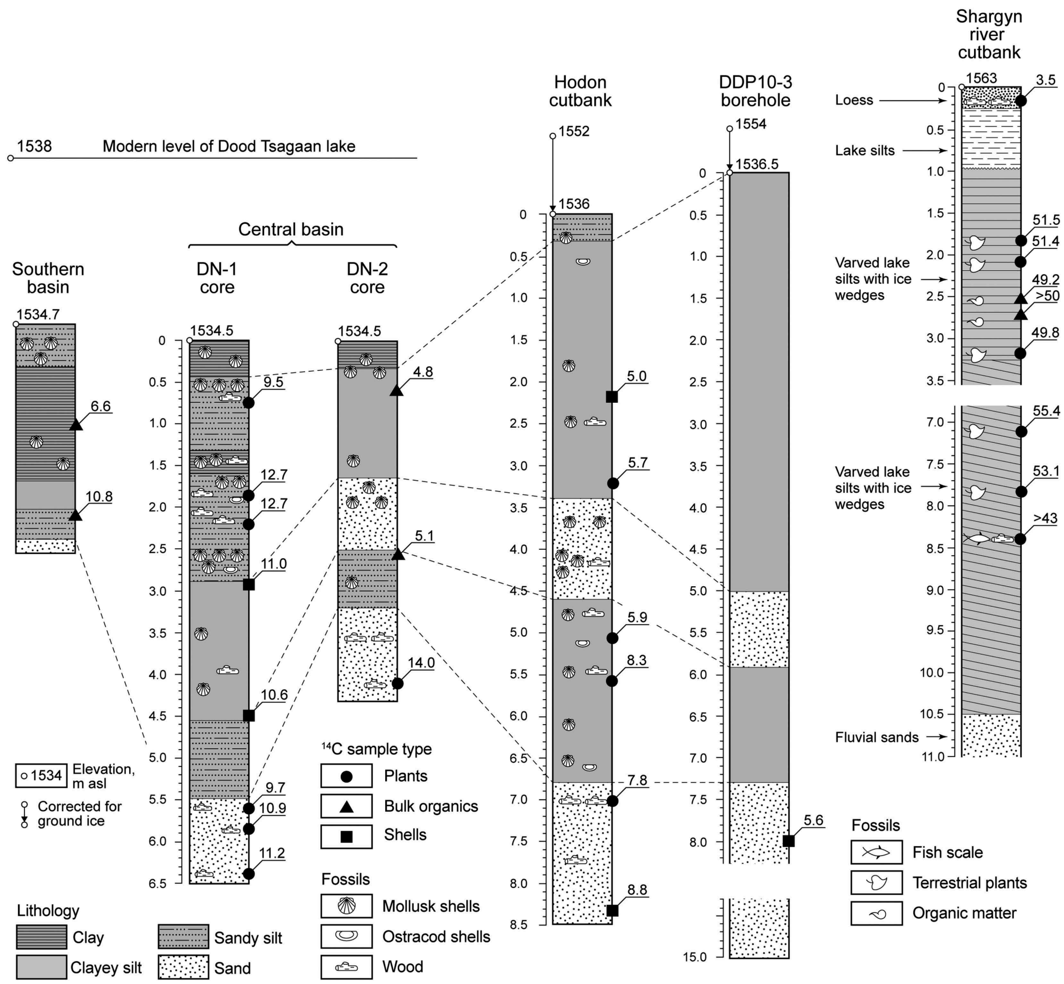

Figure 9. Stratigraphic relationship of post-LGM sediments between the studied outcrops and the boreholes. All the ^{14}C ages (cal ka BP) are recalibrated and corrected for hard-water effects. The ages from the southern basin of Dood Tsagaan lake are from Dorofeyuk and Tarasov (1998). The sediments in the Hodon river cutbank, the boreholes DN-1, DN-2, and DDP10-3 were all dated by Krivonogov *et al*. (2012). Narantsetseg *et al*. (2013) provided two ages for DN-2 and constructed the stratigraphic correlations. Note that the Shargyn river cutbank is located at a higher elevation and not aligned to the other records (data from Gillespie *et al*. 2008).

Narantsetseg *et al*. (2013) that Darhad basin was largely dry then. They correlated the stratigraphy of the DN-1 and DN-2 cores with the records from the Hodon cutbank and the DDP10-3 core (Figure 9), and subdivided the sediments younger than 10 ka into four units with approximate boundaries at 8.5, 7.8, and 5.8 ka. However, the corrected ^{14}C ages for DN-1 were statistically indistinguishable over the entire ~6 m of the core, and the boundaries of the subdivision of Dood Tsagaan lake sediments largely relied on the ages from the Hodon cutbank. Therefore, the ages for the boundaries of sediment units in the DN-1 core are imprecise.

The suggestion of a dry Darhad basin at ~9 ka by Krivonogov *et al*. (2012) and Narantsetseg *et al*. (2013) appears to conflict with the establishment by Gillespie *et al*. (2008) of a deep lake up to ~1600 m asl at about the same time. There are two ways to resolve this dilemma: first, the uncertainties in dating allow for the rapid drainage of the 1600 m asl lake, followed by lengthy subaerial exposure; or second, some of the Hodon ages may be greater than the age of deposition such that the dilemma is only apparent. The Hodon cutbank is located at the junction of Shargyn, Jarai, and Hodon rivers, in a flat plain that is susceptible to deposition of lake sediments eroded from the basin upstream. Therefore, it is possible that Darhad basin was filled to 1600 m asl in the early Holocene, consistent with the post-glacial outwash plains of the Tengis river at 1606 m asl blocking the Maly Yenisei and impounding the lake.

The Shargyn river cutbank (Figure 8; 1563 m asl) exposes another deep section (~13 m) of lake sediments in Darhad basin. Two charcoal samples from its uppermost 25 cm aeolian layer were dated to ~3.5 cal ka BP (Gillespie *et al*. 2008). A prominent unconformity separates this top layer from the underlying varved lake sediments, which Gillespie *et al*. (2008) correlated to the ~10–11 ka lake sediments on Jarai moraines. These early Holocene sediments unconformably sit on dark rhythmite, probably varved, lake sediments. Eleven organic samples taken from these lake sediments at depths of ~2–8 m gave ages from ~38 cal ka BP to more than 50 cal ka BP (MIS 3 or older). A direct IRSL dating of lake sediments in the Shargyn cutbank at 9 m depth gave ages of 40.9 ± 10.8 ka, consistent with the ^{14}C ages. Because most of the likely varves at the Shargyn river are ~0.6 cm thick, the whole 10 m sequence exposed in the cutbank may represent <2000 years, much less than the scatter of the ages, and Gillespie *et al*. (2008) attributed this to residual reservoir effects, carbon exchange, and contamination. No MIS 2 lake sediments were found at the Shargyn river cutbank.

In 2004, a 92.6 m-deep core (DBC1) was drilled in the depocentre of Darhad basin, and Gillespie *et al*. (2005) provided its first description. Preliminary results of luminescence dating of the core revealed MIS 2 lake sediments from a depth of ~9 m (Batbaatar *et al*. 2008, 2009), but they admitted that the large uncertainty in the age required further analysis. Krivonogov *et al*. (2008) sampled this same core and took 11 samples from depths of 3–17 m. One sample of plant remains at a depth of ~16 m yielded an age of ~18.8 cal ka BP. The remaining 10 seemed either too old or too young to Krivonogov *et al*. (2008), which they blamed on sample contamination after the extraction; those ages were therefore not reported. The DBC1 core was later described by Krivonogov *et al*. (2012), who proposed another age model for the upper 50 m of the core, based on the palaeomagnetic reversals identified by visually matching the magnetic inclination curve for the DBC1 core and the magnetic field palaeo-intensity record from marine sediments (Channell *et al*. 2009). The palaeomagnetic age model of Krivonogov *et al*. (2012) gives a sedimentation rate of ~0.34 m ka^{-1} and ages that agree with a final deep lake during MIS 3. The model, however, assumes a constant rate of sedimentation, which is not supported by the evidence from the core itself due to the existence of many breaks in sedimentation (Batbaatar *et al*. 2012), as was acknowledged by Krivonogov *et al*. (2012).

The latest drilling in Darhad basin, ~10 km west of the town of Renchinlhumbe, reached a depth of 163.8 m (DDP10-3: Figure 8), and Krivonogov *et al*. (2012) reported an age of ~5.6 cal ka BP for gastropod shells found at a depth of ~8 m. The full results of the DDP10-3 core are not published yet.

3.2. Chronology of glacial advances in and around Darhad basin

Gillespie *et al*. (2008) radiometrically dated (^{10}Be) glacial deposits around Darhad basin in order to establish the glacial chronology there and to estimate the age of the Tengis glaciers thought to have impounded the deep palaeolakes. Other studies have reported glacial ages for the surrounding mountains. In this section we examine those published ages, recalibrated for current estimates of ^{10}Be production rates. The recalibration in general raises the ages by no more than 15% and does not greatly affect the chronology, but it is important to have the most accurate ^{10}Be ages if they are to be compared to other radiometric dates, such as ^{14}C and luminescence.

We also report estimated equilibrium-line altitudes (ELA) for the dated advances to help in regional correlation. Over a region as small as Darhad basin, ELAs for the surrounding glaciers during the same glaciation should be consistent within measurement error (e.g. ~100 m: Gillespie 1991). Verifying that ELAs are the same for palaeoglaciers thought to have been coeval is helpful as a check on local chronologies, because of the possibility of 'geologic' errors in dating, such as unrecognized burial or exhumation histories of individual samples. This is especially a risk in permafrost-prone areas affected by solifluction, now or in the past.

In this review we consider glaciers related to the East Sayan ice field and other mountains surrounding Darhad basin, and Otgontenger peak in the central massif of Mongolia, 300 km south of Darhad. The summary of the recalculated ^{10}Be ages previously published is given in Table 6 and Figure 10. To constrain the chronology of glacial advances in the mountains bordering Darhad basin, Gillespie *et al*. (2008) sampled 22 granitic boulders sitting on moraines and outwash in the Tengis, Jarai, and Högiin river valleys (Figure 8) and measured CRE ages from their ^{10}Be. The bedrock wind gap east of the Tengis river at 1638 m asl was once a spillway of an ice-marginal stream into a Darhad palaeolake, and two exotic boulders there were dated to ~21 and 24 ka. These ages may have been younger than the 1710 m asl highstand, but showed that an MIS 2 glacier was at least within ~3 km of blocking the outlet from Darhad basin.

There was considerable variability in the ages of boulders from the moraines. In Tengis valley, upstream from the Yenisei/Tengis confluence, the ages for three of the four dated boulders were ~28–35 ka; the fourth was younger at ~17 ka. Only one of the four postdated MIS 3. Taken together, the six samples from the Tengis valley suggest that the outlet glaciers in the Tengis

Table 6. Published and recalculated ^{10}Be ages for glacial deposits in and around Darhad basin.

Sample identification	Latitude N/Longitude E (decimal degrees)	Elevation (m asl)	Sample description	Published ages (ka ± 1σ)	Recalculated ages (ka ± 1σ)	Increase in the published ages (%)	References
Tengis river, bedrock (basalt) overflow channel, the Maly Yenisei exit from Darhad basin							Gillespie *et al.* (2008)
081400-arg-Tin-01	51.479217/99.055533	1638	Quartzite boulder	19.2 ± 1.3	21.3 ± 1.3	10	
081400-arg-Tin-01b	51.479217/99.055533	1638	Granite boulder	21.6 ± 1.5	23.9 ± 1.5	10	
Tengis river, ground till and recessional outwash, the Maly Yenisei exit from Darhad basin							Gillespie *et al.* (2008)
081700-rmb-Tin-01a	51.650383/99.118083	1729	Granite boulder	31.2 ± 2.2	34.5 ± 2.2	10	
081700-rmb-Tin-01c	51.650383/99.118083	1729	Quartzite boulder	25.3 ± 1.7	28.0 ± 1.7	10	
Tengis river, ground till & recessional outwash at Uzgen lake, the Maly Yenisei exit from Darhad basin							Gillespie *et al.* (2008)
081700-arg-Uzg-002d	51.624200/99.189100	1932	Dacite boulder	15.6 ± 1.1	16.8 ± 1.1	7	
081700-arg-Uzg-003	51.624200/99.189100	1932	Granitic boulder	27.7 ± 2.0	30.5 ± 2.0	9	
Jarai river, older right-lateral piedmont moraines, Darhad basin							Gillespie *et al.* (2008)
080900-arg-Gar-la-001	51.399567/99.772200	1633	Granitic boulder	21.4 ± 1.5	23.7 ± 1.5	10	
080900-arg-Gar-la-002	51.399567/99.772200	1633	Granitic boulder	19.0 ± 1.3	21.1 ± 1.3	10	
081000-arg-Gar-la-003	51.399567/99.772200	1633	Granitic boulder	21.7 ± 1.5	25.1 ± 1.5	13	
081000-arg-Gar-la-010	51.399567/99.772200	1633	Granitic boulder	40.9 ± 2.7	45.4 ± 2.7	10	
081000-arg-Gar-la-011	51.399567/99.772200	1633	Granitic boulder	40.3 ± 4.1	44.7 ± 4.1	10	
081000-arg-Gar-la-012	51.399567/99.772200	1633	Granitic boulder	17.6 ± 1.2	19.5 ± 1.2	10	
081000-arg-Gar-la-013	51.399567/99.772200	1633	Granitic boulder	18.3 ± 1.3	20.3 ± 1.3	10	
Jarai river, younger right-lateral piedmont moraines, Darhad basin							Gillespie *et al.* (2008)
081000-arg-Gar-lla-005	51.399350/99.799900	1676	Granitic boulder	27.4 ± 1.9	30.4 ± 1.9	10	
081000-arg-Gar-lla-007	51.399350/99.799900	1676	Granitic boulder	16.8 ± 1.1	18.6 ± 1.1	10	
081000-arg-Gar-lla-008	51.399350/99.799900	1676	Granitic boulder	19.3 ± 1.3	21.4 ± 1.3	10	
Högiin river pre-MIS 2 left-lateral kame(?), Darhad basin							Gillespie *et al.* (2008)
082100-arg-Huj-01a	51.005767/99.141450	1716	Granitic boulder	221.4 ± 19.2	246.9 ± 19.2	10	
082100-arg-Huj-01b	51.005767/99.141450	1716	Granitic boulder	100.8 ± 6.7	111.9 ± 6.7	10	
082100-arg-Huj-01c	51.005767/99.141450	1716	Granitic boulder	128.5 ± 8.6	142.8 ± 8.6	10	
Högiin river end moraine, Darhad basin							Gillespie *et al.* (2008)
082100-arg-Huj-02c	50.981700/99.145800	1679	Granitic boulder	14.9 ± 1.1	16.5 ± 1.1	10	
082100-arg-Huj-02d	50.981700/99.145800	1679	Granitic boulder	40.9 ± 2.8	45.3 ± 2.8	10	
082100-arg-Huj-02e	50.981700/99.145800	1679	Granitic boulder	26.3 ± 1.9	29.1 ± 1.9	10	
Sentsa river valley terminal moraine, East Sayan mountains							Arzhannikov *et al.* (2012)
S07BE6	52.680400/99.506750	1443	Granitic boulder	16.1 ± 3.2	18.1 ± 3.2	11	
S07BE7	52.682430/99.509000	1445	Granitic boulder	18.2 ± 1.4	20.6 ± 1.4	11	
S07BE8	52.682460/99.508750	1453	Granitic boulder	16.0 ± 1.5	18.1 ± 1.5	11	
S07BE9	52.682730/99.509050	1453	Granitic boulder	15.4 ± 1.3	17.4 ± 1.3	11	
Jombolok river terminal moraine front, East Sayan mountains							Arzhannikov *et al.* (2012)
S07BE10	52.752210/99.708550	1293	Granitic boulder	23.2 ± 1.9	26.4 ± 1.9	12	
S07BE11	52.752130/99.707250	1294	Granitic boulder	21.4 ± 1.8	24.3 ± 1.8	12	
S07BE12	52.752500/99.705080	1294	Granitic boulder	22.1 ± 2.8	25.0 ± 2.8	12	
Jombolok river valley terminal moraine, East Sayan mountains							Arzhannikov *et al.* (2012)
S07BE13	52.740030/99.633030	1420	Granitic boulder	23.9 ± 1.9	27.0 ± 1.9	11	
S07BE14	52.739800/99.633183	1420	Granitic boulder	23.0 ± 2.5	26.0 ± 2.5	11	
S07BE15	52.739700/99.633370	1413	Granitic boulder	39.3 ± 3.6	44.4 ± 3.6	12	
Sailag river terminal moraine, East Sayan mountains							Arzhannikov *et al.* (2012)
S07BE16	52.777116/99.718416	1383	Granitic boulder	62.1 ± 5.7	70.2 ± 5.7	12	
S07BE17	52.777683/99.718616	1385	Granitic boulder	15.0 ± 1.4	17.0 ± 1.4	12	
S07BE18	52.778333/99.721216	1385	Granitic boulder	16.0 ± 1.6	18.1 ± 1.6	11	

(*Continued*)

Table 6. (Continued).

Sample identification	Latitude N/Longitude E (decimal degrees)	Elevation (m asl)	Sample description	Published ages (ka ± 1σ)	Recalculated ages (ka ± 1σ)	Increase in the published ages (%)	References
Recessional moraines of the southern outlet glacier, Otgontenger, Hangai mountains							Rother *et al.* (2014)
MON-D-II-I	47.6789/97.2083	2084	Granite boulder	15.3 ± 1.8	16.6 ± 1.0	8	
MON-D-II-II	47.6791/97.2084	2082	Granite boulder	15.2 ± 1.3	16.5 ± 1.0	8	
MON-D-II-III	47.6780/97.2097	2094	Granite boulder	29.9 ± 3.6	33.5 ± 2.0	11	
MON-D-IV-I	47.6883/97.2496	2150	Granite boulder	19.6 ± 2.4	21.6 ± 1.3	9	
MON-D-IV-II	47.6881/97.2505	2150	Granite boulder	17.0 ± 1.5	18.7 ± 1.1	9	
MON-D-IV-III	47.6881/97.2505	2151	Granite boulder	13.8 ± 1.7	15.0 ± 0.9	8	
Left lateral moraines of the southern outlet glacier, Otgontenger, Hangai mountains							Rother *et al.* (2014)
MON-F-I-I	47.6699/97.2618	2243	Granite boulder	23.9 ± 2.9	26.8 ± 1.7	11	
MON-F-I-II	47.6698/97.2618	2272	Granite boulder	25.3 ± 3.1	28.5 ± 1.7	11	
MON-F-I-IV	47.6734/97.2723	2300	Granite boulder	20.9 ± 2.5	23.4 ± 1.4	11	
Right lateral moraines of the southern outlet glacier, Otgontenger, Hangai mountains							
MON-E-III-I	47.7147/97.2808	2269	Bedrock	17.3 ± 2.1	19.2 ± 1.2	10	
MON-E-III-II	47.7153/97.2815	2274	Granite boulder	17.1 ± 2.1	18.9 ± 1.2	10	
MON-E-III-III	47.7164/97.2824	2277	Granite boulder	16.8 ± 2.0	18.6 ± 1.1	10	
Terminal moraines of the southern outlet glacier, Otgontenger, Hangai mountains							Rother *et al.* (2014)
MON-D-I-I	47.6835/97.2098	2140	Granite boulder	39.8 ± 4.8	45.1 ± 2.7	12	
MON-D-I-II	47.6837/97.2099	2133	Granite boulder	20.3 ± 2.5	22.4 ± 1.4	9	
MON-D-I-III	47.6836/97.2098	2137	Granite boulder	37.1 ± 4.5	41.9 ± 2.6	12	
Terminal moraines pushed up the side valley from the northern outlet glacier, Otgontenger, Hangai mountains							Rother *et al.* (2014)
MON-E-I-I	47.8498/97.3333	2568	Granite boulder	36.9 ± 4.5	42.9 ± 2.6	14	
MON-E-I-II	47.8598/97.3334	2563	Granite boulder	50.7 ± 6.2	59.5 ± 3.6	15	
MON-E-I-III	47.8597/97.3336	2560	Granite boulder	27.7 ± 3.6	31.9 ± 2.4	13	
MON-E-II-I	47.8595/97.3159	2580	Granite boulder	54.2 ± 6.6	63.5 ± 4.0	15	
MON-E-II-II	47.8587/97.3199	2596	Granite boulder	20.8 ± 2.5	23.6 ± 1.5	12	
MON-E-II-III	47.8584/97.3217	2600	Granite boulder	34.5 ± 4.2	40.1 ± 2.5	14	

The ^{10}Be ages were recalculated using CRONUS-Earth version 2.2 (Balco *et al.* 2008) with the calibrated ^{10}Be production rate of 3.99 ± 0.22 atoms g^{-1} year^{-1} (Heyman 2014) when referenced to the scaling of Stone (2000). Gillespie *et al.* (2008) used CRONUS-Earth version 1.2 with a production rate of 5.2 atoms g^{-1} year^{-1} and adopted the scaling of Lal (1991) corrected for palaeomagnetic variation, which is called Lm scheme of Lal (1991)/Stone (2000). Arzhannikov *et al.* (2012) reported using the production rate of 4.49 ± 0.29 atoms g^{-1} year^{-1}; Rother *et al.* (2014) used 4.43 ± 0.52 atoms g^{-1} year^{-1} referenced to Dunai scaling (Dunai 2001). For consistency we accepted only the ages with the scaling of Stone (2000) without palaeomagnetic correction, because the uncertainty of the ages from the other scaling schemes did not exceed the margin of analytical error (see online supplementary material for calculations with alternative scaling schemes). We used 2.7 g cm^{-3} for sample density (same value used in Gillespie *et al.* 2008), instead of 2.5 g cm^{-3} in Arzhannikov *et al.* (2012) and 2.6 g cm^{-3} in Rother *et al.* (2014). Using 2.6 g cm^{-3} would make less than 0.3% difference in the apparent age for samples <10 cm thick. No burial history and erosion was assumed in the recalculation of the ^{10}Be ages.

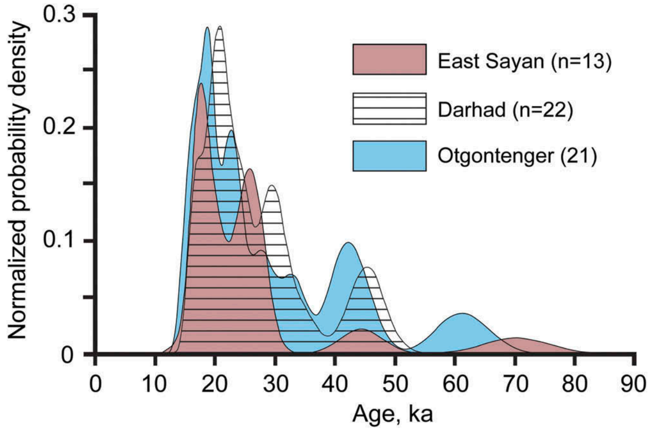

Figure 10. Summed normal distribution density of ^{10}Be cosmic-ray exposure ages discussed in this article. The East Sayan mountain group includes the 13 ages from Jombolok, Sentsa, and Sailag river valleys (Arzhannikov *et al.* 2012). The Darhad basin group includes the 22 ages from Gillespie *et al.* (2008). The 21 ages for the Otgontenger mountain are from Rother *et al.* (2014). Colour version is available online.

valley likely dammed the Maly Yenisei during MIS 3, and MIS 2 glaciers may have done so too.

A different outlet glacier from the East Sayan ice field advanced down the Jarai river valley and left two sets of piedmont moraines on the eastern side of Darhad basin. Seven of the ten ^{10}Be ages for these moraines scattered from ~19–25 ka (MIS 2); the other three (30–45 ka) predated MIS 2. Gillespie *et al.* (2008) attributed this scatter to inherited ^{10}Be. These moraines postdated the 1710 m asl highstand of the palaeolake, but were themselves inundated to 1679 m asl, and on the strength of these ages Gillespie *et al.* (2008) argued that the latest deep palaeolakes dated from MIS 2, provided that the Jarai glaciers advanced synchronously with the damming Tengis glaciers.

South of the Maly Yenisei and on the western side of Darhad basin, the Ulaan Taiga ice cap fed glaciers in the Högiin valley. Three samples from an older remnant of a left-lateral moraine or kame terrace significantly predated MIS 2, ranging from ~112 to 247 ka. A younger glacier terminated on a palaeolake shore at ~1670 m asl; it yielded three ages of 17, 29, and 45 ka.

The mountains around Hövsgöl basin, another extensional basin in the Baikal rift east of Darhad, also hosted Pleistocene glaciers. An outlet glacier from the East Sayan ice field advanced to Hövsgöl basin through the Bayan Zürhiin ranges along the Ih Horoo river valley (Figure 8), where Wegmann *et al.* (2011) dated granite boulders from two end moraines on the piedmont. Two of six ^{10}Be samples from the lower end moraine postdated MIS 2 at ~9 and 12 ka and one predated MIS 2 at ~32 ka. The remaining three clustered from 20 to 25 ka. Five kilometres up-valley, Wegmann *et al.* (2011) dated six boulders from the other end moraine. Two of the ^{10}Be ages were 28 and 23 ka; the remaining four were from 14 to 16 ka. These ages were calculated using the out-of-date 'default' ^{10}Be production rate of the CRONUS calculator (Balco *et al.* 2008), and in their abstract Wegmann *et al.* (2011) did not provide the analytical data necessary to recalculate new ages using the revised rate. Recalculation with the new production rate of Heyman (2014) increased the published ages of Gillespie *et al.* (2008) in Darhad basin by no more than 15%. Recalculation of the ages of Wegmann *et al.* (2011) should lead to a similar increase, but that is not enough to change their interpretation here.

North of Darhad basin, Arzhannikov *et al.* (2012) dated sequences of moraines left by outlet glaciers advancing to the northeast from the East Sayan ice field (Figure 4). At the Jombolok river valley a total of five ^{10}Be samples from the two sets of terminal moraines yielded an average MIS 2 age of ~24 ka, excluding an additional older sample at ~45 ka. They also dated four boulders from moraines of the neighbouring Sentsa river valley, ~8 km southwest of the Jombolok moraines. These had an average age of ~18 ka. Arzhannikov *et al.* (2012) also dated three boulders from the terminal moraines of the Sailag river valley, also neighbouring the Jombolok valley. Two of the three ^{10}Be ages averaged ~18 ka; the third was significantly older at ~74 ka and may have been reworked from an older exposure. Arzhannikov *et al.* (2012) interpreted their findings to show that the local LGM advances in the East Sayan occurred during MIS 2. This is consistent with the timing of the Jarai moraines in Darhad basin, as documented by Gillespie *et al.* (2008).

About 320 km southwest of Darhad basin, the Hangai mountains (Figure 2), were also extensively glaciated during the Pleistocene, with multiple ice fields. One was centred north of Otgontenger peak, which is still capped by a firn field today. Rother *et al.* (2014) dated six samples from end moraines at ~2590 m asl to ~38 ka (MIS 3) where an outlet glacier pushed up a side valley. A younger terminal moraine, at a lower elevation of ~2500 m asl, did not reach as far (~1.5 km) up the side valley as the MIS 3 moraines. Rother *et al.* (2014) regarded this as MIS 2 based on its minimal erosion. In the nearby valley of a different outlet glacier, three boulders from the lateral moraines were dated to ~26 ka. In the valley floor, five of six boulders from recessional moraines were dated to ~18 ka and the sixth, probably anomalous, to ~34 ka.

3.2.1. Equilibrium line altitudes

In this review, the main use of dating is to establish the timing of the glacier dams that impounded the palaeolake sources of the giant outburst floods down the Maly Yenisei. The available dating provides an imperfect chronology, because despite the effort invested the area is large, and also because natural geologic disturbances such as reworking, cryoturbation, and exhumation of dated boulders have led to variability in measured CRE ages, even from boulder to boulder on the same moraine. In establishing a regional chronology, it is necessary to know which moraines belong to the same advance, so that the ages can be grouped. If the regional ELA depression is similar for the dated moraines, that is an aid in their correlation.

Together, the studies cited above give a preliminary glacial chronology, but it is necessary to ask what degree of spatial coherence may be expected for glacial advances and retreats over the region, such as would be necessary if the chronology were used to determine the ages of impounded palaeolakes in Darhad basin. This is because the temporal patterns of glacier expansion/retreat and ELA depression in Central Asia have been shown to differ from place to place (Gillespie and Molnar 1995). For example, Koppes *et al*. (2008) reported that the global LGM (MIS 2) glaciers in Kyrgyz Tien Shan were limited to the cirques when mountain glaciers in Europe and North America advanced to their maximum extents. A similar pattern was observed in northeastern Tibet, where the last maximum glacial advances occurred during MIS 3 (Heyman *et al*. 2011). Modelling experiments by Rupper *et al*. (2009) suggested that the ELA differences in Central Asia are largely due to spatially and temporally variable snowfall amounts in the arid, cold setting, although in warmer areas melting may be the limiting factor.

If the ELAs and ages show are consistent across the region, including Darhad basin, this increases confidence in the application of the grouped chronology to estimate the extent of the Tengis glaciers and the timing of the dams, not yet dated directly. To do this, it is necessary to determine local values for the empirical coefficients in the ELA calculations.

Gillespie *et al*. (2008) calculated, by comparison to the maximum elevation of well-preserved lateral moraines, a local toe-to-headwall altitude ratio (THAR) of 0.58 for the Hoit Aguy massif to estimate the ELA of the glaciers of Darhad basin. Although the MIS 3 glaciers were larger than the MIS 2 glaciers around Darhad basin, their corresponding ELAs were no more than ~75 m lower than for the MIS 2 glaciers (ELA ~2300 m asl). Gillespie *et al*. (2008) interpreted these ages and ELAs around Darhad basin to indicate that the Tengis glaciers during both MIS 2 and MIS 3 were large enough to dam Darhad basin; however, Krivonogov *et al*. (2012) regarded this conclusion regarding MIS 2 as an open question.

For the Ih Horoo advances, we estimate the ELAs to be ~2320 and ~2300 m asl, consistent with the ELAs in Darhad basin. We calculated the ELAs for Jombolok and Sailag glaciers at 2030–2230 m asl, also consistent with the Darhad values. The dated moraines of the Otgontenger area were left by palaeo-outlet glaciers from ice caps, complicating the estimation of ELAs. We defined the ELA as the elevation of the highest lateral moraines. The highest lateral moraines in the Otgontenger area detectable from Google Earth are at ~2760 m asl, higher than near Darhad, as is consistent with their more southerly latitudes. These lateral moraines were themselves not dated, but the MIS 3 lateral moraines that were dated are found ~90 m above the dated MIS 2 moraines consistently in different valleys. The relative differences between the MIS 2 and MIS 3 moraines are about the same as in Darhad basin. Thus, direct dating of glacial deposits in the East Sayan and central Mongolia shows that in both areas the local LGM occurred during the MIS 3, but the MIS 2 glaciers were only slightly less extensive. Furthermore, the ELAs of the same age appear to change over this entire region only with latitude, such that the composite chronology is likely applicable to the Tengis glaciers.

4. Discussion

Large gravel dunes in the Kyzyl basin, high flood terraces in Tuva, and the evidence of deep lakes in Darhad basin are all evidence of cataclysmic floods down the Maly Yenisei river. The largest of the floods on Earth as measured by estimated peak discharge – the Missoula floods of Washington State, USA, and the floods from the Kuray-Chuya basin in the Russian Altai – were initiated after the breaching of glacier dams at the end of the global LGM during MIS 2 (e.g. Bretz 1969; Reuther *et al*. 2006). The size of the Darhad floods also implies a deep dam that was suddenly breached, and glacial ice is the most likely candidate, especially considering the apparent absence of landslide headwall scarps of sufficient size to block the Maly Yenisei to the necessary depth. However, the existence of a higher glacier dam does not preclude lower outwash or alluvium dams created during glacier retreat, and such appear to have existed at the mouth of the Tengis river.

Komatsu *et al*. (2009) used numerical modelling to simulate a flood from palaeolake Darhad assuming a surface level at 1710 m asl, which equates to a 172 m-deep lake with a volume of ~373 km^3. This is not the deepest palaeolake in Darhad basin (~1825 m asl) but it is the best documented, and the most likely to correspond to preserved landforms downstream. The dam was assumed to have been glacial ice that failed instantaneously. In the modelled hydrograph, the discharge peaked at ~3.5×10^6 m^3 s^{-1} within 10 minutes of the initial breach. Water depth remained high (50–100 m) in the gorges north of Ulaan Taiga long after the initial surge (Figure 11). The floodwaters would have travelled more than 100 km in 20 hours, and past the Kyzyl basin within 80 hours.

The second highest stand of Darhad palaeolake at 1710 m asl requires impounding by glacier ice, likely the Tengis glacier. The age of this palaeolake was MIS 3 given the fossil evidence and dating from the Shargyn river cutbank. It may have refilled to the roughly same level during MIS 2, but this cannot be confirmed definitely by the available ages. Grosswald (1987) used the evaporation rate of the Volga river basin and modern annual precipitation in Darhad basin to estimate that the basin could be refilled within 100–130 years to 1720 m asl. Krivonogov *et al.* (2005) roughly estimated that it would take 285 years to fill Darhad basin to a level of 1700 m asl, at a rate of ~0.35 m $year^{-1}$ adjusted from the modern value for the runoff in Hövsgöl basin. From the shorelines on the dated Jarai moraines, it does appear that a deep MIS 2 palaeolake did occupy Darhad basin at least to 1679 m asl.

The dated boulders on the wind gaps east of the Tengis river suggest the MIS 2 glacier approached the Maly Yenisei within 2 km. The dating of the flood-eroded end moraines in the Sarig valley should determine whether the Tengis glacier crossed the Maly Yenisei during MIS 2, but will not indicate the depth of the palaeolake. Beach sands exist at high elevations in Darhad basin, for example at ~1670 m asl near Arsain river, and direct dating of these deposits should constrain the timing of the deeper lake.

The deep permafrost encountered in the cores of Ufland *et al.* (1971) and in the core DBC1 (Gillespie *et al.* 2005) in Darhad basin suggested to Krivonogov *et al.* (2012) that the basin was largely dry and not shielded by the lake from sub-zero temperatures since MIS 3, enough time to develop permafrost. This argument requires an assumption that the MIS 2 lake was continuous and of long duration. However, the unconformities in the sediment stratigraphy, such as the lake sediments separated by thin peat layers at Shargyn cutbank (Gillespie *et al.* 2008), suggest that frequent draining of the palaeolakes occurred, which presents less of a thermal barrier to the formation and preservation of permafrost. In addition, there is no quantitative justification of the assumption that Darhad basin was filled during all or most of MIS 2, since the necessary dating has yet to be conducted.

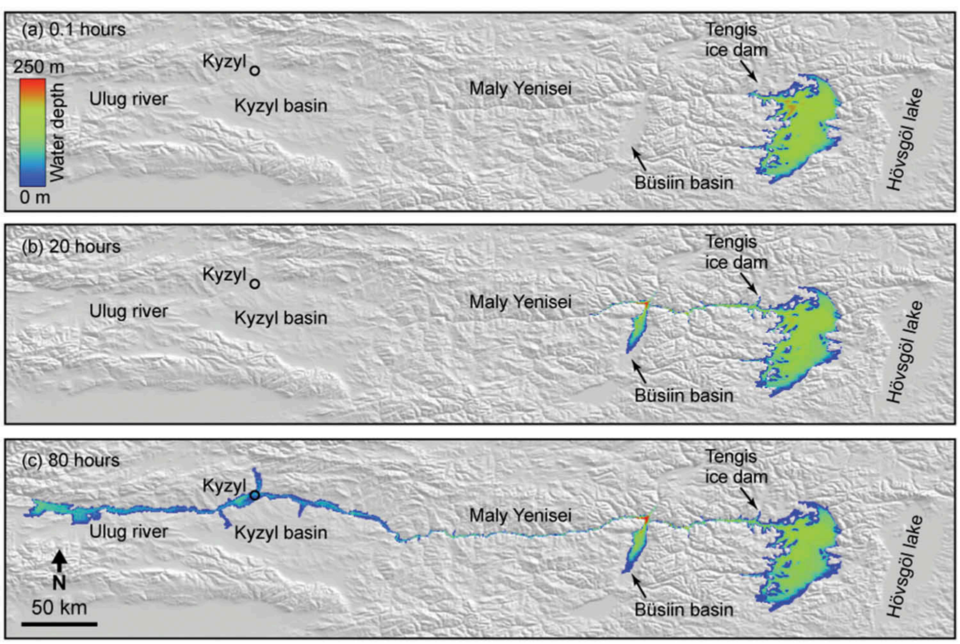

Figure 11. Inundation map of a flood from the Darhad palaeolake with surface level at 1710 m asl, adapted from Komatsu *et al.* (2009). The background is the shaded-relief image from the SRTM DEM. Due to limited computing power, they used a low-resolution DEM from the US Geological Survey (927 × 598 m grids) in which the elevation of the Büsiin basin was underestimated. The DEM also had other artefacts, such as striping in Darhad basin, and their numerical model may have overestimated the water depth at some locations (G. Komatsu, pers. comm., 2015).

Direct dating of lake sediments in Darhad basin is, so far, restricted to outcrops in the basin and short cores extracted from the modern lake floors. The controversy identified by Krivonogov *et al*. (2012) regarding the existence of a deep MIS 2 lake was raised mostly because no lake sediments from the time period were found in the incomplete sections from the cutbanks. The absence of evidence, however, is not a certain indication that the sediments were in fact not deposited. The Shargyn river cutbank, for example, is located closer to the edge of Darhad basin, where we speculate that rapid draining of the putative MIS 2 palaeolakes may have locally scoured and removed the uppermost lake sediments (e.g. Lamb and Fonstad 2010). More complete records of lake sediments may be buried in the centre of the basin, which may be less susceptible to erosion. Deep drilling in the basin may be required to establish a more complete record of lake sediments.

There may have been smaller floods along the Maly Yenisei from Darhad and other basins. For example, partial draining of the palaeolakes through the Tengis glacier dam may have occurred via subglacial tunnelling, flotation, partial collapse of the glacier front, or overtopping, especially when the glacier dam was low during advance or retreat.

To the best of our knowledge, direct dating of flood deposits along the Maly Yenisei has not been conducted. Luminescence or radiocarbon dating of gravel dunes in the Kyzyl basin and the sediments capping the basalt terraces near Darhad basin should help determine the timing and the corresponding floodwater level.

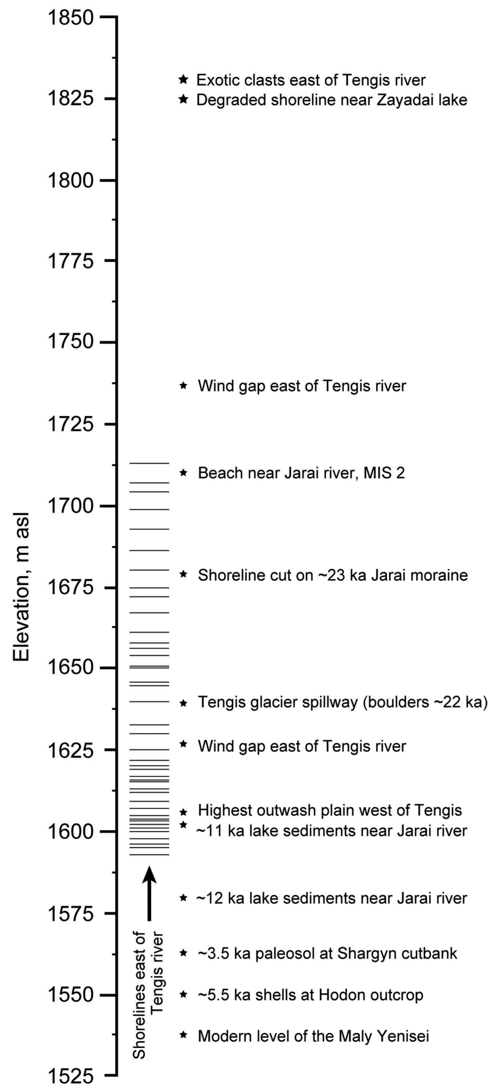

Figure 12. Shorelines and highstands of Darhad palaeolakes. Elevation of shorelines east of the Tengis river was measured by Krivonogov *et al*. (2005). The shells at Hodon outcrop were analysed by Krivonogov *et al*. (2012). The ages from Jarai, Tengis, and Shargyn rivers are from Gillespie *et al*. (2008).

5. Summary

The banks of the Maly Yenisei preserve sediments transported by many floods of various origins. The largest of them were from outburst floods originated from Darhad basin. The timing of the highstands of the Darhad palaeolakes is derived from either dating beach sands having measured elevations, from dating moraines upon which shorelines have been eroded, or from dating glacial deposits near the spillway for which ice thicknesses have been estimated. The shoreline elevations and available ages are summarized in Figure 12.

The outlet glaciers from the East Sayan ice field blocked Darhad basin at least twice during the late Pleistocene (19–22 ka, MIS 2, and ~35–53 ka, MIS 3). Direct dating of moraines suggests that Darhad basin hosted a 180 m-deep lake during the local LGM, which was likely during MIS 3. Shoreline features and glacial deposits found in Darhad basin at 1825 m asl, above the MIS 3 shoreline, suggest that greater floods may have occurred earlier. These events may have happened during MIS 6, but no detailed study confirms this possibility.

Despite the widespread evidence of cataclysmic floods along the Maly Yenisei, and recent advancements in the CRE and luminescence dating methods, there have been few detailed studies of the flood sediments and their ages over the broad geographic region affected by the floods. Such future studies might allow us to improve our understanding of the temporal relationships between palaeolakes, dams, and flood deposits in the Maly Yenisei.

This literature review is Part I of a two-part article on the cataclysmic floods of the Maly Yenisei. Part II presents new chronological evidence that resolves the question of the existence of an MIS 2 lake in Darhad basin, impounded by the Tengis glacier.

Note

1. $H = 0.086D^{1.19}$. H – Dune height, in m; D – Water depth, in m.

Acknowledgements

We thank Guest Editors Alexei Ivanov, Victor Baker, and Sergey Arzhannikov for inviting this article for the Special Issue, and we thank Alexei Ivanov, B. Charlotte Schreiber, and James Shulmeister for carefully reading the manuscript. We are grateful to Goro Komatsu and Robin Beebee for constructive and helpful critical formal reviews. We thank Bud Burke and Joanna Redwine for helpful discussions.

Disclosure statement

No potential conflict of interest was reported by the authors.

Funding

This work was supported by the Quaternary Research Center and the Department of Earth and Space Sciences, University of Washington.

ORCID

J. Batbaatar http://orcid.org/0000-0001-7806-8361

References

Allen, J.R.L., 1968, Current ripples: Their relation to patterns of water and sediment motion: Amsterdam, North-Holland Pub. Co., 433 p.

Arzhannikov, S.G., Alexeev, S.V., Glyzin, A.V., Razmakhnina, T.B., and Orlova, L.A., 2000, Prirodnaya obstanovka v golotsene zapadnoi chasti Todzhinskoi vpadiny (na primere razreza Merzly Yar) (Natural conditions in the western part of the Todzhinsky basin in the Holocene (by the example of "Merzly Yar" section)), *in* The Problems of Climatic and Environmental Reconstruction in the Holocene and Pleistocene of Siberia, Novosibirsk, IAET Publishing, Russian Academy of Sciences, p. 18–29. (in Russian)

Arzhannikov, S.G., Braucher, R., Jolivet, M., Arzhannikova, A.V., Vassallo, R., Chauvet, A., Bourlès, D., and Chauvet, F., 2012, History of late Pleistocene glaciations in the central Sayan-Tuva Upland (southern Siberia): Quaternary Science Reviews, v. 49, p. 16–32. doi:10.1016/j.quascirev.2012.06.005

Baker, V.R., 1973, Paleohydrology and sedimentology of Lake Missoula flooding in Eastern Washington: Geological Society of America Special Paper, v. 144, p. 1–79.

Baker, V.R., 1982, The channels of Mars: Austin, Texas, University of Texas Press, 198 p.

Baker, V.R., Benito, G., and Rudoy, A.N., 1993, Paleohydrology of Late Pleistocene Superflooding, Altay Mountains, Siberia: Science, v. 259, p. 348–350. doi:10.1126/science.259.5093.348

Baker, V.R., and Milton, D.J., 1974, Erosion by catastrophic floods on Mars and Earth: Icarus, v. 23, p. 27–41. doi:10.1016/0019-1035(74)90101-8

Balco, G., Briner, J., Finkel, R.C., Rayburn, J.A., Ridge, J.C., and Schaefer, J.M., 2009, Regional beryllium-10 production rate calibration for late-glacial northeastern North America: Quaternary Geochronology, v. 4, p. 93–107. doi:10.1016/j.quageo.2008.09.001

Balco, G., Stone, J.O., Lifton, N.A., and Dunai, T.J., 2008, A complete and easily accessible means of calculating surface exposure ages or erosion rates from ^{10}Be and ^{26}Al measurements: Quaternary Geochronology, v. 3, p. 174–195. doi:10.1016/j.quageo.2007.12.001

Batbaatar, J., Feathers, J.K., and Gillespie, A.R., 2009, IRSL feldspar dates for paleolake sediments from Darhad Basin, Mongolia: Geological Society of America, Abstracts with Programs, v. 41, no. 7, p. 382.

Batbaatar, J., Gillespie, A.R., Fedotov, A., and Bayasgalan, A., 2008, The 92-m sediment core from paleolake Darhad, Mongolia, *in* Proceedings, The 7th International Symposium on Environmental Changes in East Eurasia and Adjacent Areas – High Resolution Environmental Records of Terrestrial Sediments, Ulaanbaatar–Hatgal, Mongolia, August 23–29: Ulaanbaatar, Institute of Geology and Mineral Resources, Mongolian Academy of Sciences, p. 66–74.

Batbaatar, J., Gillespie, A.R., and Schreiber, B.C., 2012, Tectonics and environment at the western end of the Baikal rift: Paleolake sediment record from Darhad Basin, northern Mongolia: Geological Society of America Abstracts with Programs, v. 44, no. 3, p. 56.

Benito, G., and O'Connor, J.E., 2003, Number and size of last-glacial Missoula floods in the Columbia River valley between the Pasco Basin, Washington, and Portland, Oregon: Geological Society of America Bulletin, v. 115, no. 5, p. 624–638. doi:10.1130/0016-7606(2003)115<0624:NASOLM>2.0.CO;2

Bohorquez, P., Carling, P.A., and Herget, J., in this issue, Dynamic simulation of catastrophic late Pleistocene glacial-lake drainage, Altai Mountains, central Asia, International Geology Review. doi:10.1080/00206814.2015.1046956

Bretz, J.H., 1923, The channeled scablands of the Columbia Plateau: The Journal of Geology, v. 31, p. 617–649. doi:10.1086/jg.1923.31.issue-8

Bretz, J.H., 1969, The Lake Missoula floods and the channeled scabland: The Journal of Geology, v. 77, no. 5, p. 505–543. doi:10.1086/jg.1969.77.issue-5

Carling, P.A., 1996, Morphology, sedimentology and palaeohydraulic significance of large gravel dunes, Altai Mountains, Siberia: Sedimentology, v. 43, p. 647–664. doi:10.1111/j.1365-3091.1996.tb02184.x

Carling, P.A., Kirkbride, A.D., Parnachov, S., Borodavko, P.S., and Berger, G.W., 2002, Late Quaternary catastrophic flooding in the Altai Mountains of south-central Siberia: A synoptic overview and introduction to flood deposit sedimentology, *in* Martini, I.P., Baker, V.R., et al., eds., Flood and Megaflood Processes and Deposits: Recent and Ancient Examples: International Association of Sedimentologists Special Publication, Volume 32: London, Blackwell Science, p. 17–35.

Carson, R.J., Gillespie, A.R., and Bayasgalan, A., 2003, Late Quaternary geology along the Högiin Gol, northern Mongolia: Proceedings of the Oregon Academy of Science, v. 39, p. 20–21.

Channell, J.E.T., Xuan, C., and Hodell, D.A., 2009, Stacking paleointensity and oxygen isotope data for the last 1.5 Myr (PISO-1500): Earth and Planetary Science Letters, v. 283, p. 14–23. doi:10.1016/j.epsl.2009.03.012

Clarke, G.K.C., Mathews, W.H., and Pack, R.T., 1984, Outburst floods from glacial Lake Missoula: Quaternary Research, v. 22, p. 289–299. doi:10.1016/0033-5894(84)90023-1

Craig, R.G., 1987, Dynamics of a Missoula flood, *in* Mayer, L., and Nash, D., eds., Catastrophic flooding: Winchester, Allen and Unwin, p.305–332.

Dorofeyuk, N.I., and Tarasov, P.E., 1998, Vegetation and levels of the lakes in the north of Mongolia during the last 12500 years, by the data of palynologic and diatom analyses: Stratigraphy and Geological Correlation, v. 6, p. 73–87.

Dunai, T., 2001, Influence of secular variation of the geomagnetic field on production rates of in situ produced cosmogenic nuclides: Earth and Planetary Science Letters, v. 193, p. 197–212. doi:10.1016/S0012-821X(01)00503-9

Farr, T.G., Rosen, P.A., Caro, E., Crippen, R., Duren, R., Hensley, S., Kobrick, M., Paller, M., Rodriguez, E., Roth, L., Seal, D., Shaffer, S., Shimada, J., Umland, J., Werner, M., Oskin, M., Burbank, D., and Alsdorf, D., 2007, The shuttle radar topography mission: Reviews of Geophysics, v. 45, no. 2, p. 1–33. doi:10.1029/2005RG000183

Fisher, T.G., 2003, Chronology of glacial Lake Agassiz meltwater routed to the Gulf of Mexico: Quaternary Research, v. 59, no. 2, p. 271–276. doi:10.1016/S0033-5894(03)00011-5

Gillespie, A.R., 1991, Testing a new climatic interpretation for the Tahoe glaciation, *in* Hall Jr., C.A., Doyle-Jones, V., and Widawski, B., eds., Natural History of Eastern California and High-Altitude Research: Proceedings of the White Mountain Research Station Symposium, Volume 3: Los Angeles, CA, University of California, p. 383–398.

Gillespie, A.R., Bayasgalan, A., and Kuharic, M.V., 2005, Sediment core from ice-dammed palaeolake Darhad, Mongolia: Geological Society of America Abstracts with Programs, v. 37, no. 7, p. 543.

Gillespie, A.R., Burke, R.M., Komatsu, G., and Bayasgalan, A., 2008, Late Pleistocene glaciers in Darhad Basin, northern Mongolia: Quaternary Research, v. 69, p. 169–187. doi:10.1016/j.yqres.2008.01.001

Gillespie, A.R., and Molnar, P., 1995, Asynchronous maximum advances of mountain and continental glaciers: Reviews of Geophysics, v. 33, p. 311–364. doi:10.1029/95RG00995

Google Earth Pro ver. 7.1.2.2041, 2015, Ulaan Taiga mountains 51.443663°N, 98.954412°E, Image source: Landsat. Accessed October, 2015.

Gravis, G.F., 1974, Kriogennoe stroenie mnogoletnemerzlykh gornykh porod (Cryogenic structure of the permafrost), *in* Melnikov, P.I., ed., Geocryological conditions of Mongolian People's Republic, Transactions of the Joint Soviet-Mongolian Scientific-Research Geological Expedition, Volume 10: Moscow, Nauka, p. 117–132. (in Russian)

Grosswald, M.G., 1965, Razvitie relyefa Sayano-Tuvinskogo nagorya (Geomorphological development of the Sayan-Tuva upland): Moscow, Nauka, 166 p. (in Russian)

Grosswald, M.G., 1987, Poslednee oledenenie Sayano-Tuvinskogo nagorya: Morfologiya, intensivnost pitaniya, podprudnye ozera (The last glaciation of the Sayany-Tuva highland: Morphology and the rate of filling of ice-dammed lakes), *in* Kotikov, V.M., and Grosswald, M.G., eds., Interaction of Glaciations with the Atmosphere and Ocean: Moscow, Nauka, p. 152–170. (in Russian)

Grosswald, M.G., 1999, Evraziiskie gidrosfernye katastrofy i oledenenie Arktiki (Cataclysmic Megafloods in Eurasia and the Polar Ice Sheets): Moscow, Nauchny Mir, 117 p. (in Russian)

Grosswald, M.G., and Rudoy, A.N., 1996a, Chetvertichnye lednikovo-podprudnye ozera v gorakh Sibiri (Quaternary ice-dammed lakes in the South Siberia mountains): Izvestiya Akademii Nauk SSSR, Seriya geograficheskaya, v. 6, p. 112–126. (in Russian)

Grosswald, M.G., and Rudoy, A.N., 1996b, Quaternary glacier-dammed lakes in the mountains of Siberia: Polar Geography, v. 20, p. 180–198. doi:10.1080/10889379609377599

Herget, J., 2005, Reconstruction of Pleistocene Ice-dammed Lake Outburst floods in the Altai Mountains, Siberia: Geological Society of America Special Paper, v. 386, p. 118 p.

Herget, J., 2012, Ice-dammed lake outburst floods in the Altai Mountains, Siberia – A review with links for further readings: Tomsk State University Journal of Biology, v. 1, no. 17, p. 148–168.

Heyman, J., 2014, Paleoglaciation of the Tibetan Plateau and surrounding mountains based on exposure ages and ELA depression estimates: Quaternary Science Reviews, v. 91, p. 30–41. doi:10.1016/j.quascirev.2014.03.018

Heyman, J., Stroeven, A.P., Caffee, M.W., Hättestrand, C., Harbor, J.M., Li, Y., Alexanderson, H., Zhou, L., and Hubbard, A., 2011, Palaeoglaciology of Bayan Har Shan, NE Tibetan Plateau: Exposure ages reveal a missing LGM expansion: Quaternary Science Reviews, v. 30, p. 1988–2001. doi:10.1016/j.quascirev.2011.05.002

Ivanov, A.V., Demonterova, E.I., He, H., Perepelov, A.B., Travin, A.V., and Lebedev, V.A., 2015, Volcanism in the Baikal rift: 40 years of active-versus-passive model discussion: Earth-Science Reviews, v. 148, p. 18–43. doi:10.1016/j.earscirev.2015.05.011

Jóhannesson, T., 2002, The initiation of the 1996 jökulhlaup from Lake Grímsvötn, Vatnajökull, Iceland, *in* Snorrason, Á., Finnsdóttir, H.P., and Moss, M., eds., The extremes of the extremes—Extraordinary floods: Wallingford, Oxfordshire, England, IAHS Press, International Association of Hydrological Sciences Publication No. 271, p. 57–64.

Komatsu, G., Arzhannikov, S.G., Arzhannikova, A.V., and Ershov, K., 2007a, Geomorphology of subglacial volcanoes in the Azas Plateau, the Tuva Republic, Russia: Geomorphology, v. 88, p. 312–328. doi:10.1016/j.geomorph.2006.12.002

Komatsu, G., Arzhannikov, S.G., Arzhannikova, A.V., and Ori, G. G., 2007b, Origin of glacial-fluvial landforms in the Azas Plateau volcanic field, the Tuva Republic, Russia: Role of ice-magma interaction: Geomorphology, v. 88, p. 352–366. doi:10.1016/j.geomorph.2006.12.003

Komatsu, G., Arzhannikov, S.G., Gillespie, A.R., Burke, R.M., Miyamoto, H., and Baker, V.R., 2009, Quaternary paleolake formation and cataclysmic flooding along the upper Yenisei River: Geomorphology, v. 104, p. 143–164. doi:10.1016/j.geomorph.2008.08.009

Komatsu, G., and Baker, V.R., 2007, Formation of valleys and cataclysmic flooding on Earth and Mars, *in* Chapman, M.G., ed., The geology of Mars: Evidence from Earth-based analogs: Cambridge, Cambridge University Press, p. 297–321.

Komatsu, G., Baker, V.R., Arzhannikov, S., Gallagher, R., Arzhannikova, A.V., Murana, A., and Oguchi, T., in this issue, Catastrophic flooding, palaeolakes and late Quaternary drainage reorganization in northern Eurasia, International Geology Review. doi:10.1080/00206814.2015.1048314

Komatsu, G., Clute, S.K., and Baker, V.R., 1997, Preliminary remote sensing assessment of Pleistocene cataclysmic floods in Central Asia, *in* Proceedings, 28th Annual Lunar and Planetary Science Conference, March 17–21: Houston, Texas, Lunar and Planetary Institute, p. 747–748.

Koppes, M., Gillespie, A.R., Burke, R.M., Thompson, S.C., and Stone, J., 2008, Late Quaternary glaciation in the Kyrgyz Tien Shan: Quaternary Science Reviews, v. 27, p. 846–866. doi:10.1016/j.quascirev.2008.01.009

Krivonogov, S.K., Kazansky, A.Y., Oyunchimeg, TS., Narantsetseg, TS., Tomurhuu, D., and Dolgorsuren, KH., 2008, New in studies of the Darhad basin, Mongolia, *in* Proceedings, the 7th International Symposium on Environmental Changes in East Eurasia and Adjacent Areas – High Resolution Environmental Records of Terrestrial Sediments, Ulaanbaatar–Hatgal, Mongolia, August 23–29: Ulaanbaatar, Institute of Geology and Mineral Resources, Mongolian Academy of Sciences, p. 90–91.

Krivonogov, S.K., Sheinkman, V.S., and Mistryukov, A.A., 2005, Ice damming of the Darhad paleolake (northern Mongolia) during the Late Pleistocene: Quaternary International, v. 136, p. 83–94. doi:10.1016/j.quaint.2004.11.010

Krivonogov, S.K., Yi, S., Kashiwaya, K., Kim, J.C., Narantsetseg, T., Oyunchimeg, T., Safonova, I.Y., Kazansky, A.Y., Sitnikova, T., Kim, J.Y., and Hasebe, N., 2012, Solved and unsolved problems of sedimentation, glaciation and palaeolakes of the Darhad Basin, Northern Mongolia: Quaternary Science Reviews, v. 56, p. 142–163. doi:10.1016/j.quascirev.2012.08.013

Lal, D., 1991, Cosmic ray labeling of erosion surfaces: In situ nuclide production rates and erosion models: Earth and Planetary Science Letters, v. 104, p. 424–439. doi:10.1016/0012-821X(91)90220-C

Lamb, M.P., and Fonstad, M.A., 2010, Rapid formation of a modern bedrock canyon by a single flood event: Nature Geoscience, v. 3, p. 477–481. doi:10.1038/ngeo894

Lyell, C., 1830–3, Principles of Geology, being an attempt to explain the former changes of the Earth's surface, by reference to causes now in operation, vols. 1–3: London, John Murray.

Malde, H.E., 1968, The catastrophic late Pleistocene Bonneville flood in the Snake River Plain, Idaho: U.S. Geological Survey Professional Paper 596: Washington, DC, United States Government Printing Office, 52 p.

Mangerud, J., Jakobsson, M., Alexanderson, H., Astakhov, V., Clarke, G., Henriksen, M., Hjort, C., Krinner, G., Lunkka, J.P., Möller, P., Murray, A., Nikolskaya, O., Saarnisto, M., and Svendsen, J.I., 2004, Ice-dammed lakes and rerouting of the drainage of Northern Eurasia during the last glaciation: Quaternary Science Reviews, v. 23, p. 1313–1332. doi:10.1016/j.quascirev.2003.12.009

Margold, M., Jansson, K.N., Stroeven, A.P., and Jansen, J.D., 2011, Glacial Lake Vitim, a 3000-km^3 outburst flood from Siberia to the Arctic Ocean: Quaternary Research, v. 76, p. 393–396. doi:10.1016/j.yqres.2011.06.009

Merle, J.R., 2001, Quaternary geology of the Tengis-Shishid Gol region, Khovsgol, Mongolia [Senior thesis]: Walla Walla, Washington, Whitman College, 56 p.

Montgomery, D.R., 2013, The Rocks Don't Lie: A Geologist Investigates Noah's Flood: New York, W. W. Norton & Company, 320 p.

Montgomery, D.R., Hallet, B., Yuping, L., Finnegan, N., Anders, A., Gillespie, A., and Greenberg, H.M., 2004, Evidence for Holocene megafloods down the Tsangpo River gorge, southeastern Tibet: Quaternary Research, v. 62, p. 201–207. doi:10.1016/j.yqres.2004.06.008

Narantsetseg, TS., Krivonogov, S.K., Oyunchimeg, TS., Uugantsetseg, B., Burr, G.S., Tomurhuu, D., and Dolgorsuren, KH., 2013, Late Glacial to Middle Holocene climate and environmental changes as recorded in Lake Dood sediments, Darhad Basin, northern Mongolia: Quaternary International, v. 311, p. 12–24. doi:10.1016/j.quaint.2013.08.043

Normark, W.R., and Reid, J.A., 2003, Extensive deposits on the Pacific Plate from Late Pleistocene North American glacial lake outbursts: The Journal of Geology, v. 111, p. 617–637. doi:10.1086/jg.2003.111.issue-6

O'Connor, J.E., and Baker, V.R., 1992, Magnitudes and implications of peak discharges from glacial Lake Missoula: Geological Society of America Bulletin, v. 104, p. 267–279. doi:10.1130/0016-7606(1992)104<0267:MAIOPD>2.3.CO;2

O'Connor, J.E., Clague, J.J., Walder, J.S., Manville, V., and Beebee, R.A., 2013, Outburst floods, *in* Shroder, J.F., ed., Treatise on geomorphology, Volume 9: San Diego, Academic Press, p. 475–510. doi:10.1016/B978-0-12-374739-6.00251-7

O'Connor, J.E., and Costa, J.E., 2004, The world's largest floods—Their causes and magnitudes: U.S. Geological Survey Circular 1254: Reston, VA, U.S. Geological Survey, 13 p.

Olyunin, V.N., 1965, Neotectonics and Glaciation of East Sayan: Moscow, Nauka, 128 p. (in Russian)

Owen, L.A., Richards, B., Rhodes, E.J., Cunningham, W.D., Windley, B.F., Badamgarav, J., and Dorjnamjaa, D., 1998, Relict permafrost structures in the Gobi of Mongolia: Age and significance: Journal of Quaternary Science, v. 13, p. 539–547.

Pardee, J.T., 1942, Unusual currents in glacial Lake Missoula, Montana: Geological Society of America Bulletin, v. 53, p. 1569–1600. doi:10.1130/GSAB-53-1569

Peck, J.A., Khosbayar, P., King, J., Fowell, S.J., Aurienbyleg, K., and Soninkhishig, N., 2001, The latest Holocene sedimentary environmental magnetic record from Lake Dood, Mongolia: EOS, v. 82, p. F337.

Putnam, A.E., Denton, G.H., Schaefer, J.M., Barrell, D.J.A., Andersen, B.G., Finkel, R.C., Schwartz, R., Doughty, A.M., Kaplan, M.R., and Schlüchter, C., 2010, Glacier advance in southern middle-latitudes during the Antarctic Cold Reversal: Nature Geoscience, v. 3, p. 700–704. doi:10.1038/ngeo962

Raney, R.K., Luscombe, A.P., Langham, E.J., and Ahmed, S., 1991, RADARSAT (SAR imaging): Proceedings of the IEEE, v. 79, no. 6, p. 839–849. doi:10.1109/5.90162

Rasskazov, S.V., Luhr, J.F., Bowring, S.A., Ivanov, A.V., Brandt, I. S., Brandt, S.B., Demonterova, E.I., Boven, A.A., Kunk, M., Housh, T., and Dungan, M.A., 2003, Late Cenozoic volcanism in the Baikal rift system: Evidence for formation of the Baikal and Khubsugul basins due to thermal impacts on the lithosphere and collision-derived tectonics: Berliner Palaobiologische Abhandlungen, v. 4, p. 33–48.

Reimer, P.J., Bard, E., Bayliss, A., Beck, J.W., Blackwell, P.G., Ramsey, C.B., Buck, C.E., Cheng, H., Edwards, R.L., Friedrich, M., Grootes, P.M., Guilderson, T.P., Haflidason, H., Hajdas, I., Hatté, C., Heaton, T.J., Hoffmann, D.L., Hogg, A.G., Hughen, K.A., Kaiser, K.F., Kromer, B., Manning, S.W., Niu, M., Reimer, R.W., Richards, D.A., Scott, E.M., Southon, J.R., Staff, R.A., Turney, C.S.M., and Plicht, J., 2013, IntCal13 and MARINE13 radiocarbon age calibration curves 0–50,000 years cal BP: Radiocarbon, v. 55, no. 4, p. 1869–1887. doi:10.2458/azu_js_rc.55.16947

Reuther, A.U., Herget, J., Ivy-Ochs, S., Borodavko, P., Kubik, P. W., and Heine, K., 2006, Constraining the timing of the most recent cataclysmic flood event from ice-dammed lakes in the Russian Altai Mountains, Siberia, using cosmogenic in situ ^{10}Be: Geology, v. 34, no. 11, p. 913–916. doi:10.1130/G22755A.1

Rother, H., Lehmkuhl, F., Fink, D., and Nottebaum, V., 2014, Surface exposure dating reveals MIS-3 glacial maximum in the Khangai Mountains of Mongolia: Quaternary Research, v. 82, p. 297–308. doi:10.1016/j.yqres.2014.04.006

Rudoy, A.N., 2002, Glacier-dammed lakes and geological work of glacial superfloods in the Late Pleistocene, Southern Siberia, Altai Mountains: Quaternary International, v. 87, p. 119–140. doi:10.1016/S1040-6182(01)00066-0

Rudoy, A.N., and Baker, V.R., 1993, Sedimentary effects of cataclysmic late Pleistocene glacial outburst flooding, Altay Mountains, Siberia: Sedimentary Geology, v. 85, p. 53–62. doi:10.1016/0037-0738(93)90075-G

Rupper, S., Roe, G., and Gillespie, A., 2009, Spatial patterns of Holocene glacier advance and retreat in Central Asia: Quaternary Research, v. 72, p. 337–346. doi:10.1016/j.yqres.2009.03.007

Ryan, W.B.F., Pitman, W.C., III, Major, C.O., Shimkus, K., Moskalenko, V., Jones, G.A., Dimitrov, P., Goriir, N., Saking, M., and Yiice, H., 1997, An abrupt drowning of the Black Sea shelf: Marine Geology, v. 138, p. 119–126. doi:10.1016/S0025-3227(97)00007-8

Selivanov, E.I., 1967, Neogene-Quaternary giant lakes in Transbaikalia and North Mongolia: Reports of the Academy of Sciences of the USSR, v. 177, p. 175–178. (in Russian)

Shang, Y., Yang, Z., Li, L., Liu, D., Liao, Q., and Wang, Y., 2003, A super-large landslide in Tibet in 2000: Background, occurrence, disaster, and origin: Geomorphology, v. 54, no. 3–4, p. 225–243. doi:10.1016/S0169-555X(02)00358-6

Sharkhuu, A., Sharkhuu, N., Etzelmüller, B., Heggem, E.S.F., Nelson, F.E., Shiklomanov, N.I., Goulden, C.E., and Brown, J., 2007, Permafrost monitoring in the Hovsgol mountain region, Mongolia: Journal of Geophysical Research, v. 112, p. F02S06. doi:10.1029/2006JF000543

Smith, L.N., 2006, Stratigraphic evidence for multiple drainings of glacial Lake Missoula along the Clark Fork River, Montana, USA: Quaternary Research, v. 66, p. 311–322. doi:10.1016/j.yqres.2006.05.009

Stone, J., 2000, Air pressure and cosmogenic isotope production: Journal of Geophysical Research, v. 105, no. B10, p. 23753–23759. doi:10.1029/2000JB900181

Stuiver, M., and Reimer, P.J., 1993, Extended ^{14}C database and revised CALIB radiocarbon calibration program: Radiocarbon, v. 35, p. 215–230.

Teller, J.T., Leverington, D.W., and Mann, J.D., 2002, Freshwater outbursts to the oceans from glacial Lake Agassiz and their role in climate change during the last deglaciation: Quaternary Science Reviews, v. 21, p. 879–887. doi:10.1016/S0277-3791(01)00145-7

US Geological Survey, 2012, Landsat – A global land-imaging mission: U.S. Geological Survey Fact Sheet, v. 2012, no. 3072, p. 3.

Ufland, A.K., Iljin, A.V., Spirkin, A.I., and Shilova, G.N., 1971, Main features of stratigraphy and formation of Cenozoic deposits in Prekosogol (MPR): Bulletin of the Moscow Society of Naturalists (MOIP). Geology Series, v. 46, p. 54–69. (in Russian)

Waitt, R.B., Jr., 1980, About forty last-glacial Lake Missoula Jökulhlaups through Southern Washington: The Journal of Geology, v. 88, p. 653–679. doi:10.1086/jg.1980.88.issue-6

Wegmann, K.W., Amgaa, TS., Frankel, K.L., Dewett, A.P., and Bayasgalan, A., 2011, Geologic, geomorphic, and environmental change at the northern termination of the Lake Hövsgöl rift, Mongolia, *in* Proceedings of the Twenty-Fourth Annual Keck Research Symposium in Geology, Union College, Schenectady, NY, April, 2011, p. 220–229.

Wiedmer, M., Montgomery, D.R., Gillespie, A.R., and Greenberg, H., 2010, Late Quaternary megafloods from glacial Lake Atna, Southcentral Alaska, U.S.A.: Quaternary Research, v. 73, p. 413–424. doi:10.1016/j.yqres.2010.02.005

Wortmann, M., Krysanova, V., Kundzewicz, Z.W., Su, B., and Li, X., 2014, Assessing the influence of the Merzbacher Lake outburst floods on discharge using the hydrological model SWIM in the Aksu headwaters, Kyrgyzstan/NW China: Hydrological Processes, v. 28, p. 6337–6350. doi:10.1002/hyp.v28.26

Yamskikh, A.F., and Yamskikh, A.A., 1999, Dynamics of the Todza ice-dammed lake (upper Yenisei River, southern Siberia) during the late Pleistocene and Holocene: Science Reports of Tohoku University, 7th Series (Geography), v. 49, no. (Special Issue on GLOCOPH 98), p. 143–159.

Yamskikh, A.F., Yamskikh, G.Y., Vasiliev, S.A., and Ermolova, N. M., 2001, Paleoecology of the Maina group of multiplayer Paleolithic sites in the Yenisei River valley (at the boundary between West Sayan Mountains and Minusa Depression): Field Guidebook for the Global Continental Paleohydrology Meeting, Krasnoyarsk-Khakassia Tuva Region, Russia, p. 146–156.

Yang, D., Ye, B., and Kane, D.L., 2004, Streamflow changes over Siberian Yenisei River Basin: Journal of Hydrology, v. 296, p. 59–80. doi:10.1016/j.jhydrol.2004.03.017

Yarmolyuk, V.V., Lebedev, V.I., Sugorakova, A.M., Bragin, V.YU., Litasov, YU.D., Prudnikov, S.T., Arakelyants, M.M., Lebedev, V.A., Ivanov, V.G., and Kozlovskii, A.M., 2001, Eastern Tuva Area of the youngest volcanism of Central Asia: Stages, products, and character of volcanic activity: Volcanology and Seismology, v. 3, p. 3–32. (in Russian)

Young, N.E., Schaefer, J.M., Briner, J.P., and Goehring, B.M., 2013, A Be-10 production rate calibration for the Arctic: Journal of Quaternary Science, v. 28, p. 515–526. doi:10.1002/jqs.v28.5